



Deposited via The University of Sheffield.

White Rose Research Online URL for this paper:

<https://eprints.whiterose.ac.uk/id/eprint/172451/>

Version: Published Version

---

**Article:**

Evans, D.J.A., Roberts, D.H., Bateman, M.D. et al. (2021) Retreat dynamics of the eastern sector of the British–Irish Ice Sheet during the last glaciation. *Journal of Quaternary Science*, 36 (5). pp. 723-751. ISSN: 0267-8179

<https://doi.org/10.1002/jqs.3275>

---

**Reuse**






This article is distributed under the terms of the Creative Commons Attribution (CC BY) licence. This licence allows you to distribute, remix, tweak, and build upon the work, even commercially, as long as you credit the authors for the original work. More information and the full terms of the licence here:

<https://creativecommons.org/licenses/>

**Takedown**

If you consider content in White Rose Research Online to be in breach of UK law, please notify us by emailing [eprints@whiterose.ac.uk](mailto:eprints@whiterose.ac.uk) including the URL of the record and the reason for the withdrawal request.

# Retreat dynamics of the eastern sector of the British–Irish Ice Sheet during the last glaciation

DAVID J. A. EVANS,<sup>1\*</sup>  DAVID H. ROBERTS,<sup>1</sup> MARK D. BATEMAN,<sup>2</sup> CHRIS D. CLARK,<sup>2</sup> ALICIA MEDIALDEA,<sup>3</sup>  LOUISE CALLARD,<sup>4</sup> ELENA GRIMOLDI,<sup>5</sup> RICHARD C. CHIVERRELL,<sup>6</sup> JEREMY ELY,<sup>2</sup>  DAYTON DOVE,<sup>7</sup> COLM Ó COFAIGH,<sup>1</sup>  MARGOT SAHER,<sup>8</sup> TOM BRADWELL,<sup>9</sup>  STEVEN G. MORETON,<sup>10</sup> DEREK FABEL<sup>11</sup> and SARAH L. BRADLEY<sup>12</sup>

<sup>1</sup>Department of Geography, Durham University, Durham, UK

<sup>2</sup>Department of Geography, University of Sheffield, Sheffield, UK

<sup>3</sup>National Research Centre on Human Evolution (CENIEH), Burgos, Spain

<sup>4</sup>School of Geography, Politics and Sociology, Newcastle University, Newcastle, UK

<sup>5</sup>Fugro, Fugro House, Wallingford, Oxford, UK

<sup>6</sup>School of Environmental Sciences, University of Liverpool, Liverpool, UK

<sup>7</sup>British Geological Survey, Lyell Centre, Herriot Watt University, Edinburgh, UK

<sup>8</sup>School of Ocean Sciences, Bangor University, Anglesey, UK

<sup>9</sup>Biological and Environmental Sciences, University of Stirling, Stirling, UK

<sup>10</sup>Natural Environment Research Council, Radiocarbon facility, East Kilbride, UK

<sup>11</sup>Scottish Universities Environmental Research Centre, East Kilbride, UK

<sup>12</sup>Institute of Geography, University of Cologne, Cologne, Germany

Received 21 April 2020; Revised 16 November 2020; Accepted 11 January 2021

**ABSTRACT:** The findings of BRITICE-CHRONO Transect 2 through the North Sea Basin and eastern England are reported. We define ice-sheet marginal oscillation between ~31 and 16 ka, with seven distinctive former ice-sheet limits (L1–7) constrained by Bayesian statistical analysis. The southernmost limit of the North Sea Lobe is recorded by the Bolders Bank Formation (L1; 25.8–24.6 ka). L2 represents ice-sheet oscillation and early retreat to the northern edge of the Dogger Bank (23.5–22.2 ka), with the Garret Hill Moraine in north Norfolk recording a significant regional readvance to L3 at 21.5–20.8 ka. Ice-marginal oscillations at ~26–21 ka resulted in L1, L2 and L3 being partially to totally overprinted. Ice-dammed lakes related to L1–3, including Lake Humber, are dated at 24.1–22.3 ka. Ice-sheet oscillation and retreat from L4 to L5 occurred between 19.7 and 17.3 ka, with grounding zone wedges marking an important transition from terrestrial to marine tidewater conditions, triggered by the opening of the Dogger Lake spillway between 19.9 and 17.5 ka. L6 relates to ice retreat under glacial conditions and final ice retreat into the Firth of Forth by 15.8 ka. L7 (~15 ka) represents an ice retreat from Bosies Bank into the Moray Firth. Copyright © 2021 The Authors *Journal of Quaternary Science* Published by John Wiley & Sons Ltd

**KEYWORDS:** British–Irish Ice Sheet; ice-sheet flow dynamics; MIS2; North Sea Lobe; palaeoglaciology

## Introduction

This paper reviews the results of the BRITICE-CHRONO Transect 2 through the North Sea Basin and onto the onshore areas of eastern England in the context of pre-existing knowledge on the behaviour of the British–Irish Ice Sheet (BIIS) in the region. It is a critical region for palaeoglaciological reconstruction because it was characterised by confluence between the BIIS and the Fennoscandinavian Ice Sheet (FIS), where ice flow was highly dynamic (and possibly surge-influenced) and ice streams appear to have switched on and off through the last glacial cycle (cf. Balson & Jeffrey 1991; Eyles *et al.* 1994; Carr *et al.* 2006; Hubbard *et al.* 2009; Sejrup *et al.* 2009, 2016; Boston *et al.* 2010; Graham *et al.* 2011; Clark *et al.* 2012). In the north and central North Sea, subglacial landforms and deposits are overlain by glacial marine sediments that record marine inundation following deglaciation. In contrast, in the south, the shallow seas of the Dogger Bank and offshore areas of Yorkshire, Lincolnshire and Norfolk contain a

record of deglaciation in a terrestrial setting, with subglacial landscapes overprinted by glacial lacustrine, glacial fluvial outwash and Holocene marine sediments (e.g. Dove *et al.* 2017; Roberts *et al.* 2018).

Recent hypotheses suggest that ice-sheet coalescence between the BIIS and FIS over the central North Sea occurred throughout the Last Glacial Maximum (LGM; 30–23 ka), but was followed by regional decoupling and rapid flow instability of the BIIS (Sejrup *et al.* 2000; Graham *et al.* 2007, 2010; Bradwell *et al.* 2008, 2019). This was triggered first by the retreat of the Norwegian Channel Ice Stream (NCIS) and second by the catastrophic northerly drainage of the Dogger Lake complex between 19 and 17.5 ka in the southern North Sea (Sejrup *et al.*, 2016). However, despite many years of work, several key questions remain unanswered. Working in the North Sea region, Transect 2 of the BRITICE-CHRONO project specifically aimed to explore several key questions: 1) how far did the BIIS extend at the LGM?; 2) how, when and where did the BIIS and FIS uncouple?; 3) did marine inundation of the northern North Sea destabilise the BIIS and thereby trigger rapid east-to-west retreat?; and 4) what were the

\*Correspondence: David J. A. Evans, as above.

E-mail: d.j.a.evans@durham.ac.uk

major BIIS controls on North Sea ice flow dynamics and deglaciation patterns?

The findings of Transect 2 are summarised here based upon new data from a number of localised case studies that were designed to further interrogate the existing glacial geomorphology, Late Quaternary stratigraphy and geochronology in key locations around the British sector of the North Sea Basin (Evans *et al.* 2017, 2018, 2019; Bateman *et al.* 2018; Roberts *et al.* 2018, 2019), as well as concurrent reports on glacial reconstructions prepared outwith, but at the same time complementary to, the BRITICE-CHRONO project (e.g. Murton *et al.* 2009; Bateman *et al.* 2008, 2015; Fairburn & Bateman 2016; Dove *et al.* 2017; Fig. 1). The findings reported in these case studies are now critically reviewed in the context of the regional reconstructions of BIIS palaeoglaciology as it pertains to the eastern margins of the ice sheet. The North Sea is subdivided into two sectors: the northern sector, extending from the Firth of Forth to the Moray Firth and east to Fladen Ground and Viking Bank/Plateau; and the southern sector, extending from the Firth of Forth to Great Fisher Bank and southwards into the southern North Sea Basin towards Dogger Bank and the Yorkshire, Lincolnshire and Norfolk coasts.

## Glacial land systems of the North Sea region

The North Sea Basin during the Late Quaternary cold stages was characterised by subaerial conditions as a result of the low stands of glacioeustatic sea levels (e.g. Waelbroeck *et al.* 2002). Chronostratigraphic control relating to this period of time is provided by the critical exposure at Sewerby, near Bridlington on the East Yorkshire coast. The stratigraphy here records beach sedimentation during Marine Isotope (MIS) Sub-Stage 5e, followed by MIS 4 periglacial colluvial and aeolian sedimentation on an exposed marine cliff and platform, and capped by the MIS 2 Skipsea Till and overlying outwash (Lamplugh 1888; Boylan 1967; Bateman & Catt 1996; Bateman *et al.* 2015). During the last cold stage, culminating in the LGM of MIS 2, it has been proposed that the BIIS and FIS coalesced, although this reconstruction has not been without controversy. Recent research has addressed the pattern and chronology of ice-sheet occupancy of the North Sea region during MIS 2, identifying complex and dynamic interaction between the FIS and the BIIS (cf. Nygård *et al.*, 2005; Carr *et al.*, 2006; Bradwell *et al.*, 2008, 2019; Sejrup *et al.*, 2009, 2015; Hjelstuen *et al.* 2018). Multiple advances and recessions, as well as ice-flow directional switches driven by shifting ice dispersal centres, have been recorded from complex glacial landform and stratigraphic assemblages related to the central BIIS (e.g. Livingstone *et al.*, 2008, 2010a, b, 2015; Davies *et al.* 2009, 2011, 2012; Evans *et al.*, 2009; Roberts *et al.* 2013) and consequently are now firmly established elements of the BIIS palaeoglaciology (cf. Clark *et al.* 2012; Livingstone *et al.*, 2012; Chiverrell *et al.* 2013; Hughes *et al.* 2014; Sejrup *et al.*, 2015).

The interaction of lobate ice streams in the central and eastern parts of the BIIS during MIS 2 is recorded by substantial arcuate moraine sequences and intervening glacial lake plains (Clark *et al.* 2004, 2012, 2018; Evans *et al.* 2005; Fig. 1). The most significant of these ice bodies is the North Sea Lobe (NSL), which flowed southwards for some 400 km from southern Scotland down the eastern margin of the North Sea Basin (Catt & Penny 1966; Boulton *et al.* 1985) to terminate in north Norfolk (Pawley *et al.* 2006; Moorlock *et al.* 2008; Roberts *et al.* 2018; Evans *et al.* 2019; Fig. 1). The NSL also coalesced with the Tweed, Tyne Gap and Stainmore ice streams, forming

ice-dammed lakes such as Lake Tyne, Lake Wear and Lake Tees during phases of ice-marginal recession (Agar 1954; Smith 1981; Plater *et al.* 2000; Davies *et al.* 2009, 2019; Livingstone *et al.* 2012, 2015; Yorke *et al.* 2012). Around the North Yorkshire Moors, ice-dammed lakes were created in Kildale and the Vale of Pickering by onshore flow of the NSL at its maximum extent during MIS 2 (Kendall 1902; Evans *et al.* 2017; Lincoln *et al.* 2017; Fig. 2). In the Vale of Pickering, the NSL plugged the valley mouth with substantial morainic topography (Filey and Flamborough moraines; Kendall 1902; Farrington & Mitchell 1951), thereby permanently reversing the flow of the River Derwent (King 1965; Evans *et al.* 2017). The most substantial lake created between the Pennine-sourced ice and the NSL existed in the Vale of York/Humber lowland region, where the 125 km long Vale of York ice lobe flowed from the Stainmore Gap and Tees lowlands to terminate within 10 km of the onshore-flowing NSL, plugging the Humber Estuary to construct the Ellingham/Ferriby/Horkstow moraine complex and thereby creating Glacial Lake Humber (Gaunt 1974, 1981; Straw 1979; Bateman *et al.* 2000, 2008, 2015, 2018; Fig. 2). Although Lake Humber highstands of up to ~30 m OD (Ordnance Datum) have been proposed (e.g. Gaunt *et al.* 1992; Fairburn & Bateman 2016), there is unequivocal evidence of glacialustrine deposits (Hemingbrough Formation) only up to 8 m OD in the Humber lowlands (Thomas 1999; Ford *et al.* 2008). Consequently, a potentially deeper lake (cf. Straw 1979) is regarded as an ephemeral feature during MIS 2 by Evans *et al.* (2018), likely because it was difficult to maintain by the NSL plugging the Humber Gap, and hence highstand Lake Humber was repeatedly terminated by catastrophic drainage in response to ice margin floatation.

Along the east coast of England, the advance of the NSL against the higher coastal topography and its competition with easterly flowing inland ice is recorded by multiple tills. Stratified intra- and inter-till beds such as those at Sandy Bay (Eyles *et al.* 1982), Whitburn (Davies *et al.* 2009) and Holderness (Evans *et al.* 1995; Evans & Thomson 2010) record both switches in ice flow provenance as well as phases of sedimentation in subglacial canal fills that in places fed into ice-marginal lakes. At some locations, multiple tills are separated by stratified sediments of subaerial origin and hence were suitable for optically stimulated luminescence (OSL) dating, best exemplified at sites like Sandsend, north of Whitby (Roberts *et al.* 2013) and Seaham, on the Durham coast (Roberts *et al.* 2019). At Sandsend the stratigraphy displays evidence of an early NSL advance in the form of a bedrock glacitectorite and till which is separated from an upper till, documenting a later readvance, by upward-coarsening stratified sediments of an ice-marginal lake and sandur. Similarly, on the Holderness lowlands, onshore oscillations of the NSL have been proposed by Evans and Thomson (2010) and Boston *et al.* (2010) based upon the regional stratigraphic architecture and through framing genetic interpretations within the principles of advance and retreat tills inherent within the ice-sheet sub-marginal sedimentation model of Boulton (1996a, b). These oscillations have often been associated with surging behaviour (e.g. Lamplugh 1911; Eyles *et al.* 1994; Boston *et al.* 2010) but the lack of a diagnostic surging land system signature (Evans & Rea 1999, 2003) has cautioned against an unequivocal classification of the NSL as a predominantly surging lobe (Evans & Thomson 2010). In addition to the two advances recorded by the Skipsea Till margin (Catt & Penny 1966; Catt 2007) and the Holderness hummocky drift (Eyles *et al.* 1994; Evans & Thomson 2010), a late stage readvance by the NSL is recorded by the Withernsea Till at Dimlington (Catt & Penny 1966). Throughout the oscillations and final recession of the NSL from the coast of eastern England, sedimentation has been dominated by

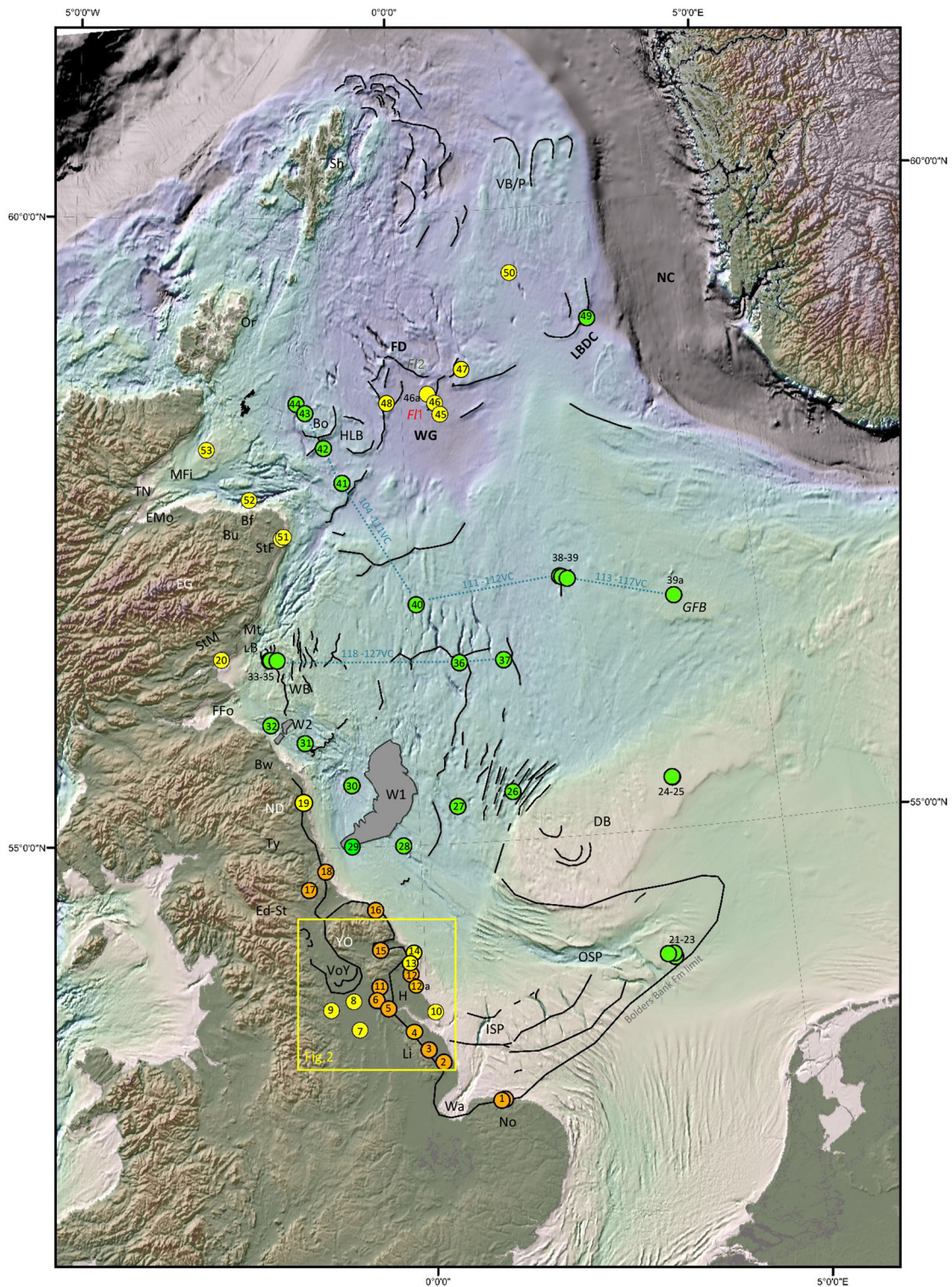


**Figure 1.** Bathymetry (EMODnet) and topography of the North Sea region, including key site locations and ice margin positions, as demarcated by moraines or the edges of till sheets (black lines) and grounding zone wedges (grey outlined areas labelled W1 and W2). Data derived from multiple published sources and BRITICE version 2 database (cf. Clark *et al.* 2018). BRITICE-CHRONO offshore and onshore sites are denoted by green and orange symbols, respectively. Legacy sites are denoted by yellow symbols. (Bf – Banff; Bw – Berwick; Bo – Bosies Bank; Bu – Buchan; DB – Dogger Bank; EG – East Grampians; EMO – East Morayshire; Ed-ST – Eden/Stainmore; Ffo – Firth of Forth; FD – Fladen deeps; F11 and F12 – Fladen Moraines; GFB – Great Fisher Bank; HLB – Halibut Bank; H – Holderness; Hu – Humber; ISP – Inner Silver Pit; Li – Lincolnshire; LBDC – Ling Bank Drainage Channel; Mfi – Moray Firth; No – Norfolk; ND – Northumberland; NC – Norwegian Channel; OSP – Outer Silver Pit; StF – St Fergus; StM – Strathmore; Wa – The Wash; TN – Tarbert Ness; TY – Tyne Gap; VoY – Vale of York; VB/P – Viking Bank/Plateau; WB – Wee Bankie; WG – Witch Ground; W1 and W2 – Grounding zone wedges; YO – Yorkshire). Onshore site locations are designated by numbers used in combination with place names in Fig. 4a and offshore site locations are designated by numbers used in combination with core names in Fig. 4b. These site numbers are used to locate dates in Table 1. Blue dashed lines represent locations of transects in Fig. 5.

the progradation and aggradation of coarse-grained subaqueous glaciallacustrine deposits (e.g. Holderness, Fig. 1; Evans & Thomson 2010) and/or ice-contact glacialfluvial deposits associated with the development of glacier karst

(e.g. Lincolnshire coastal lowlands; Evans *et al.* 2019). This has provided numerous suitable targets for OSL dating (see Table 1 and references therein), which are critically reviewed below as part of a regional palaeoglaciological reconstruction.

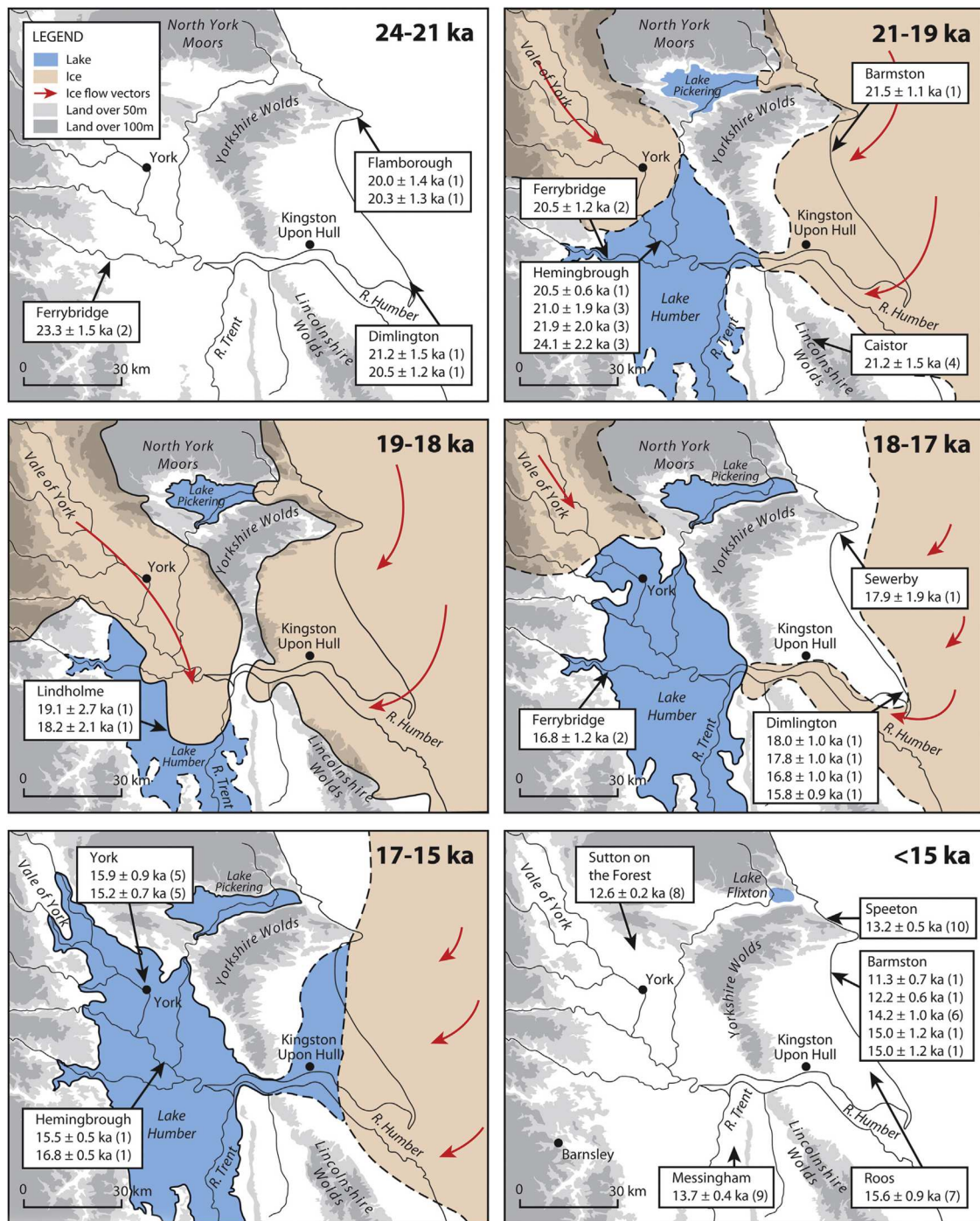


**Figure 2.** Palaeoglaciology of East Yorkshire and Vale of York/Humber Lowlands (from Bateman *et al.* 2015), showing the relative ice movements of the Vale of York and North Sea lobes of the BIIS. Ice margins are illustrative only and are based, where available, on dated stratigraphic and geomorphic evidence indicating either ice-free or ice-inundated conditions. Within time slices, ice margins may have moved significantly from that shown. Lake Humber margins are based on those of Fairburn and Bateman (2016) and for simplicity do not show internal emergent high ground. Lake Pickering extent is based on Clark *et al.* (2004) with the vestige (Lake Flixton) based on Palmer *et al.* (2015). Ages are based on OSL and radiocarbon dates and are from the following sources (bracketed numbers following ages in location boxes): 1. Bateman *et al.* (2015); 2. Bateman *et al.* (2008); 3. Murton *et al.* (2009); 4. Bateman *et al.* (2000); 5. Fairburn and Bateman (2016); 6. Allen (1980); 7. Beckett (1981); 8. Matthews (1970); 9. Bateman *et al.* (2001); 10. Straw (1979).

Recent investigations on the floor of the North Sea have identified significant landform-sediment assemblages that are critical to the reconstruction of the former dynamics and oscillations of the NSL during MIS 2 in offshore locations (Fig. 1; Dove *et al.* 2017; Roberts *et al.* 2018, 2019; Emery *et al.* 2019). In the central North Sea, the prominent feature of the Dogger Bank has been heavily glacetected, which Phillips *et al.* (2017) relate to complex thrust moraine construction by a dynamic NSL margin during MIS 2 ice-sheet recession. The shallow seafloor to the west and southwest of the Dogger Bank also contains evidence of

several later phases of ice advance and retreat related to the flow of the NSL along the depression located between the Dogger Bank and the Yorkshire/Lincolnshire coasts down to north Norfolk. Roberts *et al.* (2018) propose that the early phases of the LGM were characterised by the interaction between the southern margin of the BIIS and Dogger Lake, located in the eastern sector of the central North Sea. This water body initiated flow instability in the NSL, which was consequently subject to rapid ice advance and retreat. In contrast, during the later stages of the LGM the flow of the NSL was restricted to the western side of the Dogger Bank

**Table 1.** Dates used in compiling the chronology of ice recession in this paper, organised from south to north. Highlights are blue for OSL, yellow for TL and green for  $^{14}\text{C}$ . Where more than one OSL measurement approach has been taken for the same sample, SA denotes single aliquot measurements and SG denotes single grain measurements.

| Site N <sup>o</sup><br>(see Fig. 1) | Site name/<br>core name       | OSL/ $^{14}\text{C}$<br>Sample code | Lat/<br>Long     | Source                     | Depth<br>(m) | Previously<br>reported<br>OSL (ka) or<br>$^{14}\text{C}$ (cal ka<br>BP) | Revised<br>or new<br>age (cal<br>ka BP) | Bayesian<br>median<br>modelled age<br>(ka) |
|-------------------------------------|-------------------------------|-------------------------------------|------------------|----------------------------|--------------|---|---|--|
| 1                                   | Garret Hill                   | Shfd15033                           | 52.954           | Roberts <i>et al.</i> 2018 | 1.1          | 21.5±1.3  |   | 21.5                                       |
| 1                                   | Garret Hill                   | Shfd15034                           | -0.974           | Roberts <i>et al.</i> 2018 | 1.5          | 22.8±1.8  |   | 22.8                                       |
| 2                                   | Thoresthorpe                  | Shfd15154                           | 53.273           | Evans <i>et al.</i> 2019   | 2.2          | 17.4±1.1  |   | 17.4                                       |
| 2                                   | Thoresthorpe                  | Shfd15155 (SG)                      | -0.189           | Evans <i>et al.</i> 2019   | 2.4          | 19.3±1.4  |   | 19.6                                       |
|                                     |                               | Shfd15155 (SA)                      |                  |                            |              | 19.3±2.2  |   | 19.6                                       |
| 3                                   | Welton-le-Wold                | Shfd13074                           | 53.374<br>-0.068 | Evans <i>et al.</i> 2019   | 3.5          | 19.5±2.6  |   | 19.5                                       |
| 4                                   | North Kelsey Road,<br>Caistor | Back 1                              | 53.494           | Bateman <i>et al.</i> 2000 | 2.9          | 22.7±1.4  | 24.1±1.5                                | 24.5                                       |
| 4                                   | North Kelsey Road,<br>Caistor | Back 2                              | -0.353           | Bateman <i>et al.</i> 2000 | 1.9          | 17.7±1.2  | 19.1±1.1                                | 19.6                                       |
| 5                                   | North Ferriby                 | Shfd13072                           | 53.712           | Bateman <i>et al.</i> 2018 | 3.4          | 21.7±2.0  | 27.0±2.2                                | 27.6                                       |
| 5                                   | North Ferriby                 | Shfd13071                           | -0.516           | Bateman <i>et al.</i> 2018 | 2.4          | 22.5±1.6  | 29.5±1.7                                | 29.5                                       |
| 5                                   | North Ferriby                 | Shfd13073                           |                  | Bateman <i>et al.</i> 2018 | 1.9          | 19.4±1.8  | 21.7±2.0                                | 21.7                                       |
| 6                                   | North Cave                    | Shfd13060                           | 53.781           | Evans <i>et al.</i> 2018   | 0.8          | 11.1±0.8  |   |  |
| 6                                   | North Cave                    | Shfd13058                           | -0.668           | Evans <i>et al.</i> 2018   | 8.0          | 37.6±3.3  | 38.6±3.3                                | 37.1                                       |
| 6                                   | North Cave                    | Shfd13059                           |                  | Evans <i>et al.</i> 2018   | 6.4          | 34.7±3.4  | 41.8±3.7                                | 37.9                                       |
| 6                                   | North Cave                    | SUERC-77600                         | 58.781           | Evans <i>et al.</i> 2018   |              | 49.0±3.6  | C14 yrs                                 |  |
| 6                                   | North Cave                    | SUERC-79023                         | -0.672           | Evans <i>et al.</i> 2018   |              | 41.6±1.4  | C14 yrs                                 |  |
| 7                                   | Lindholme                     | Shfd10072                           | 53.545           | Bateman <i>et al.</i> 2015 | 1.2          | 19.1±2.7  | 19.9±3.4                                | 21.9                                       |
| 7                                   | Lindholme                     | Shfd10071                           | -0.930           | Bateman <i>et al.</i> 2015 | 0.95         | 18.2±2.1  | 18.9±3.0                                | 18.9                                       |
| 8                                   | Hemingbrough                  | Shfd11093                           | 53.776           | Bateman <i>et al.</i> 2015 | 14.1         | 20.5±0.6  | 22.3±0.7                                | 22.0                                       |
| 8                                   | Hemingbrough                  | Shfd11087                           | -0.977           | Bateman <i>et al.</i> 2015 | 1.9          | 16.8±0.5  | 19.2±0.5                                | 19.6                                       |
| 8                                   | Hemingbrough                  | Shfd11088                           |                  | Bateman <i>et al.</i> 2015 | 2.6          | 15.5±0.5  | 18.0±0.6                                | 18.0                                       |
| 8                                   | Hemingbrough                  | HEMA01                              | 53.775           | Murton <i>et al.</i> 2009  | 1.5          | 21.9±2.0  |   | 21.9                                       |
| 8                                   | Hemingbrough                  | HEMA02                              | -0.976           | Murton <i>et al.</i> 2009  | 40           | 21.0±1.9  |   | 21.9                                       |
| 8                                   | Hemingbrough                  | HEMA03                              |                  | Murton <i>et al.</i> 2009  | 4.0          | 24.1±2.2  |   | 24.1                                       |
| 9                                   | Ferrybridge                   | Shfd02012                           | 53.713           | Bateman <i>et al.</i> 2008 | 1.1          | 16.6±1.2  | 19.0±1.4                                |  |
| 9                                   | Ferrybridge                   | Shfd02014                           | -1.286           | Bateman <i>et al.</i> 2008 | 1.2          | 20.5±1.2  | 20.1±1.2                                | 21.2                                       |
| 9                                   | Ferrybridge                   | Shfd02013                           |                  | Bateman <i>et al.</i> 2008 | 2.6          | 23.3±1.5  | 24.4±1.6                                | 24.5                                       |
| 10                                  | Dimlington                    | Shfd07113 (SA)                      | 53.673           | Bateman <i>et al.</i> 2015 | 21.6         | 17.8±1.0  | 21.2±1.2                                | 21.1                                       |
|                                     |                               | Shfd07113 (SG)                      | -0.103           |                            |              | 16.9±0.9  | 20.2±1.2                                | 21.2                                       |
| 10                                  | Dimlington                    | Shfd07114 (SA)                      |                  | Bateman <i>et al.</i> 2015 | 20.8         | 17.6±0.9  | 21.0±1.1                                | 21.2                                       |
|                                     |                               | Shfd07114 (SG)                      |                  |                            |              | 18.0±0.9  | 21.5±1.1                                | 21.2                                       |
| 10                                  | Dimlington                    | Shfd07115 (SG)                      |                  | Bateman <i>et al.</i> 2015 | 20.0         | 15.7±0.8  | 18.8±1.0                                | 18.8                                       |
| 10                                  | Dimlington                    | Shfd07116 (SA)                      |                  | Bateman <i>et al.</i> 2015 | 18.7         | 17.0±0.9  | 20.3±1.1                                | 21.1                                       |
|                                     |                               | Shfd07116 (SG)                      |                  |                            |              | 17.7±1.0  | 21.2±1.1                                | 21.2                                       |
| 10                                  | Dimlington                    | Shfd09062 (SG)                      |                  | Bateman <i>et al.</i> 2015 | 26.0         | 21.1±1.4  | 23.501.5                                | 21.2                                       |
| 10                                  | Dimlington                    | Shfd09063 (SG)                      |                  | Bateman <i>et al.</i> 2015 | 26.0         | 20.5±1.2  | 22.8±1.4                                | 21.2                                       |
| 10                                  | Dimlington                    | Birm-108                            | 53.673           | Penny <i>et al.</i> 1969   | -            | 21.8±0.3  |   | 21.9                                       |
| 10                                  | Dimlington                    | I-3372                              | -0.109           | Penny <i>et al.</i> 1969   | -            | 21.9±0.4  |   | 22.0                                       |
| 11                                  | Catwick/Gembling              | Shfd13064                           | 53.886           | Bateman <i>et al.</i> 2018 | 6.3          | 22.8±1.8  | 23.5±1.8                                | 23.1                                       |
| 11                                  | Catwick/Gembling              | Shfd13065                           | -0.623           | Bateman <i>et al.</i> 2018 | 2.0          | 23.4±1.7  | 23.6±1.7                                | 23.1                                       |
| 12                                  | Barmston                      | Shfd10213                           | 54.016           | Bateman <i>et al.</i> 2015 | 4.7          | 11.3±0.7  | 12.0±0.7                                | -  |
| 12                                  | Barmston                      | Shfd10214 (SA)                      | -0.215           | Bateman <i>et al.</i> 2015 | 2.1          | 15.0±1.0  | 18.0±1.1                                | 19.6                                       |
|                                     |                               | Shfd10214 (SG)                      |                  |                            |              | 15.0±1.2  | 17.6±1.4                                | -  |
| 12                                  | Barmston                      | Shfd10215 (SA)                      |                  | Bateman <i>et al.</i> 2015 | 7.5          | 18.6±1.4  | 20.4±1.6                                | 20.2                                       |
|                                     |                               | Shfd10215 (SG)                      |                  |                            |              | 21.5±1.6  | 23.6±1.9                                | 23.6                                       |
| 12                                  | Barmston                      | Shfd10216                           |                  | Bateman <i>et al.</i> 2015 | 4.7          | 12.2±0.6  | 12.9±0.7                                | -  |
| 12                                  | Barmston                      | Shfd11007 (SA)                      |                  | Bateman <i>et al.</i> 2015 | 1.7          | 16.4±1.0  | 20.4±1.6                                | 20.4                                       |
|                                     |                               | Shfd11007 (SG)                      |                  |                            |              | 15.0±1.2  | 17.5±1.4                                | -  |
| 12a                                 | Skipsea                       | Shfd13069                           | 53.979           | Bateman <i>et al.</i> 2018 | 7.0          | 16.5±1.0  | 18.3±1.2                                | 18.3                                       |
| 12a                                 | Skipsea                       | Shfd13070                           | -0.199           | Bateman <i>et al.</i> 2018 | 6.0          | 15.9±1.3  | 17.6±1.4                                | 17.6                                       |
| 13                                  | Sewerby                       | Shfd05250                           | 54.115<br>-0.168 | Bateman <i>et al.</i> 2015 | 3.75         | 17.9±1.9  | 18.6±1.9                                | 19.6                                       |

(Continued)

Table 1. (Continued)

|     |                                       |                   |                  |                             |                 |           |          |                    |
|-----|---------------------------------------|-------------------|------------------|-----------------------------|-----------------|-----------|----------|--------------------|
| 14  | Flamborough                           | Shfd10084         | 53.104           | Bateman <i>et al.</i> 2015  | 18.4            | 20.0±1.4  | 20.9±1.4 | 21.9               |
| 14  | Flamborough                           | Shfd10085         | -0.119           | Bateman <i>et al.</i> 2015  | 6.7             | 20.3±1.3  | 21.1±1.3 | 21.9               |
| 15  | East Heslerton                        | Shfd13054         | 54.178           | Evans <i>et al.</i> 2017    | 8.6             | 17.6±1.0  | 18.4±1.0 | 19.6               |
| 15  | East Heslerton                        | Shfd13055         | -0.597           | Evans <i>et al.</i> 2017    | 5.5             | 17.3±1.0  | 18.4±1.0 | 19.6               |
| 15  | East Heslerton                        | Shfd13056         |                  | Evans <i>et al.</i> 2017    | 2.0             | 15.8±0.90 | 16.9±1.0 | -                  |
| 15  | East Heslerton                        | Shfd13057         |                  | Evans <i>et al.</i> 2017    | 1.0             | 10.1±0.7  | 11.0±0.8 | -                  |
| 16  | Sandsend                              | Shfd13068         | 54.495           | This paper                  | 12.0            |           | 23.4±1.7 | 23.1               |
| 16  | Sandsend                              | Shfd13067         | -0.647           | This paper                  | 16.8            |           | 26.1±2.1 | 26.1               |
| 16  | Sandsend                              | Shfd13066         |                  | This paper                  | 21.8            |           | 23.8±1.8 | 23.1               |
| 18  | Seaham                                | Shfd14064         | 54.811           | Roberts <i>et al.</i> 2019  | 5.4             | 19.8±1.8  |          | 19.0               |
| 18  | Seaham                                | Shfd14065         | -1.313           | Roberts <i>et al.</i> 2019  | 7.4             | 19.1±1.9  |          | 19.0               |
| 18  | Seaham                                | Shfd14066         |                  | Roberts <i>et al.</i> 2019  | 8.0             | 19.9±2.3  |          | 19.0               |
| 17  | Maiden Castle,<br>Durham City         | Shfd14067         | 54.668           | This paper                  | 2.7             |           | 16.2±0.8 | 16.2               |
| 17  | Maiden Castle,<br>Durham City         | Shfd14068         | -1.544           | This paper                  | 1.0             |           | 10.1±1.2 | -                  |
| 20  | Tay/Forth Estuary<br>(Shiells)        | SRR-391           | 56.279<br>-3.164 | Harkness & Wilson<br>1979   | -               | 16.4±0.2  |          | 16.0               |
| 20  | Tay/Forth Estuary<br>(Gallowflat)     | AA-37787          | 56.374<br>-3.276 | Peacock 2002                | Loc 3,<br>Div B | 16.7±0.1  |          | 16.7               |
| 20  | Tay/Forth Estuary<br>(Inchcoonans)    | Beta-111508       | 56.397<br>-3.231 | Peacock 2002                | No.3,<br>Div A  | 16.0±0.1  |          | 16.0               |
| 20  | Tay/Forth Estuary<br>(Gallowflat)     | CAMS-77912        | 56.374<br>-3.276 | Peacock 2002                | Loc 3,<br>Div B | 16.8±0.1  |          | 16.9               |
| 20  | Tay/Forth Estuary<br>(Barry Clay Pit) | OxA-1704          | -2.736<br>-2.736 | Hedges <i>et al.</i> 1989   | -               | 16.9±0.2  |          | 16.8               |
| 22  | North Sea 178VC                       | Shfd15179         | 54.013<br>3.351  | Roberts <i>et al.</i> 2018  | 0.15            | 25.8±2.4  |          | 27.2               |
| 23  | North Sea 179VC                       | Shfd15180         | 54.012<br>3.271  | Roberts <i>et al.</i> 2018  | 0.25            | 31.7±2.1  |          | 31.7               |
| 24  | North Sea 150VC                       | Shfd15175         | 55.405           | Roberts <i>et al.</i> 2018  | 0.16            | 29.5±1.9  |          | 29.5               |
| 25  | North Sea 151VC                       | Shfd15176         | 3.544            | Roberts <i>et al.</i> 2018  | 0.13            | 26.2±2.1  |          | 27.3               |
| 26  | North Sea 155VC                       | Shfd15178         | 55.386<br>1.319  | Roberts <i>et al.</i> 2018  | 0.35            | 23.1±2.3  |          | 23.1               |
| 27  | North Sea 137VC                       | UCIAMS-<br>176372 | 55.293<br>0.542  | Roberts <i>et al.</i> 2019  | 5.52            | 19.8±0.2  |          | 19.9               |
| 30  | North Sea 132VC                       | SUERC-68010       | 55.491<br>-0.919 | Roberts <i>et al.</i> 2019  | 1.44            | 19.6±0.2  |          | 19.4               |
| 32  | North Sea 128VC                       | SUERC-68009       | 55.979<br>-2.040 | Roberts <i>et al.</i> 2019  | 2.80            | 17.0±0.2  |          | 16.9               |
| 33  | North Sea 118VC                       | SUERC-68001       | 56.495           | Roberts <i>et al.</i> 2019  | 2.40            | 17.9±0.2  |          | 17.9               |
| 33  | North Sea 118VC                       | SUERC-68007       | -2.046           | Roberts <i>et al.</i> 2019  | 2.40            | 16.6±0.2  |          | 16.6               |
| 34  | North Sea 119VC                       | SUERC-68883       | 56.494<br>-2.029 | This paper                  | 2.00            |           | 18.0±0.2 | 19.7               |
| 35  | North Sea 120VC                       | SUERC-68008       | 56.492<br>-1.938 | This paper                  | 0.43            |           | 17.6±0.2 | 18.0               |
| 39a | North Sea 117VC                       | SUERC-72877       | 56.835<br>3.814  | This paper                  | 0.20            |           | 13.4±0.1 | Not in<br>Bayesian |
| 40  | North Sea 111VC                       | SUERC-68000       | 56.904<br>0.088  | This paper                  | 3.44            |           | 17.6±0.2 | 18.8               |
| 42  | North Sea 106VC                       | SUERC-67993       | 58.167           | This paper                  | 4.66            |           | 14.5±0.3 | 14.5               |
| 42  | North Sea 106VC                       | SUERC-67997       | -1.192           | This paper                  | 5.36            |           | 15.1±0.2 | 15.4               |
| 43  | North Sea 105VC                       | SUERC-67992       | 58.448<br>-1.460 | This paper                  | 1.55            |           | 15.1±0.2 | 15.1               |
| 44  | North Sea 104VC                       | SUERC-67990       | 58.522           | This paper                  | 2.55            |           | 15.1±0.2 | 15.1               |
| 44  | North Sea 104VC                       | SUERC-67991       | -1.590           | This paper                  | 3.23            |           | 15.2±0.1 | 15.2               |
| 45  | Fladen/Witch Ground<br>-BH 04/01      | Ua- 32760         | 58.403<br>0.577  | Graham <i>et al.</i> (2010) | 17.70           | 19.6±0.4  |          | 18.3               |
| 45  | Fladen/Witch Ground<br>-BH 04/01      | Ua-32761          |                  | Graham <i>et al.</i> (2010) | 17.70           | 16.8±0.5  |          | 16.8               |
| 46  | Fladen/Witch Ground<br>-BGS 77/2      | Ua-831            | 58.492           | Sejrup <i>et al.</i> (1994) | 8.98            | 17.5±0.3  |          | 17.7               |
| 46  | Fladen/Witch Ground<br>-BGS 77/2      | TUa-149           | 0.505            | Sejrup <i>et al.</i> (1994) | 9.00            | 23.1±0.3  |          | 23.1               |

(Continued)

Table 1. (Continued)

|     |  |             |                  |  |       |           |                    |
|-----|--|-------------|------------------|--|-------|-----------|--------------------|
| 46  | Fladen/Witch Ground<br>-BGS 77/2       | TUa-276     |                  | Sejrup <i>et al.</i> (1994)                          | 12.70 | 18.0±0.2  | 17.9               |
| 46  | Fladen/Witch Ground<br>-BGS 77/2       | TUa-458     |                  | Sejrup <i>et al.</i> (1994)                          | 16.40 | 21.3±0.2  | 21.3               |
| 46  | Fladen/Witch Ground<br>-BGS 77/2       | TUa-459     |                  | Sejrup <i>et al.</i> (1994)                          | 17.55 | 17.7±0.2  | 17.7               |
| 46  | Fladen/Witch Ground<br>-BGS 77/2       | TUa-141     |                  | Sejrup <i>et al.</i> (1994)                          | 18.00 | 19.5±0.3  | 19.5               |
| 46a | Fladen/Witch Ground<br>-BGS 58+00/ 111 | OxA-1317    | 58.567<br>0.402  | Long <i>et al.</i> 1986<br>Hedges <i>et al.</i> 1988 | 2.4   | 15.9±0.3  | 15.9               |
| 46a | Fladen/Witch Ground<br>-BGS 58+00/ 111 | OxA-1318    |                  | Long <i>et al.</i> 1986<br>Hedges <i>et al.</i> 1988 | 2.8   | 25.2±0.4  | 25.2               |
| 46a | Fladen/Witch Ground<br>-BGS 58+00/ 111 | OxA-1319    |                  | Long <i>et al.</i> 1986<br>Hedges <i>et al.</i> 1988 | 4.0   | 16.7±0.3  | 16.7               |
| 46a | Fladen/Witch Ground<br>-BGS 58+00/ 111 | OxA-1320    |                  | Long <i>et al.</i> 1986<br>Hedges <i>et al.</i> 1988 | 5.2   | 15.6±0.2  | 15.7               |
| 46a | Fladen/Witch Ground<br>-BGS 58+00/ 111 | OxA-1321    |                  | Long <i>et al.</i> 1986<br>Hedges <i>et al.</i> 1988 | 5.2   | 15.9±0.2  | 15.9               |
| 47  | Fladen<br>GS140-05-15GC                | Beta-226955 | 58.926<br>0.803  | Sejrup <i>et al.</i> (2015)                          | 1.10  | 14.2±0.1  | 14.2               |
| 47  | Fladen<br>GS140-05-15GC                | Beta-226956 |                  | Sejrup <i>et al.</i> (2015)                          | 1.36  | 14.6±0.2  | 14.6               |
| 48  | Fladen<br>GS140-05-14GC                | Beta-225422 | 58.578<br>0.726  | Sejrup <i>et al.</i> (2015)                          | 1.68  | 16.8± 0.1 | 16.8               |
| 48  | Fladen<br>GS140-05-14GC                | Beta-225420 |                  | Sejrup <i>et al.</i> (2015)                          | 1.80  | 15.6±0.1  | 15.6               |
| 48  | Fladen<br>GS140-05-14GC                | Beta-225418 |                  | Sejrup <i>et al.</i> (2015)                          | 2.01  | 16.0±0.1  | 16.0               |
| 48  | Fladen<br>GS140-05-14GC                | Beta-216741 |                  | Sejrup <i>et al.</i> (2015)                          | 2.46  | 16.2±0.1  | 16.1               |
| 49  | North Sea 097VC                        | SUERC-67989 | 59.083<br>2.913  | This paper   | 4.07  | 14.5±0.3  | Not in<br>Bayesian |
| 50  | North Sea B2001                        | TUa-274     | 58.390<br>1.728  | Sejrup <i>et al.</i> (1994)                          |       | 37.0±0.7  | Not in<br>Bayesian |
| 51  | St Fergus, Aberdeen<br>coast           | Beta-101953 | 57.471<br>-1.816 | Peacock 1999   |       | 17.1±0.1  | Not in<br>Bayesian |
| 51  | St Fergus, Aberdeen<br>coast           | Lu-3028     | 57.456<br>-1.852 | Hall and Jarvis 1989                                 |       | 17.6±0.3  | Not in<br>Bayesian |
| 52  | Moray Firth – core<br>73/35            | SRR-322     | 57.767<br>-2.317 | Harkness & Wilson<br>1979                            | -     | 19.3±0.9  | 18.8               |
| 52  | Moray Firth – core<br>73/35            | SRR-323     |                  | Harkness & Wilson<br>1979                            | -     | 19.7±0.7  | 19.3               |
| 52  | Moray Firth – core<br>73/35            | SRR-324     |                  | Harkness & Wilson<br>1979                            | -     | 17.0±0.7  | 16.5               |
| 52  | Moray Firth – core<br>73/35            | SRR-325     |                  | Harkness & Wilson<br>1979                            | -     | 20.2±0.8  | 19.7               |
| 53  | Moray Firth – core<br>74/18            | SRR - 627   | 58.167<br>-2.950 | Harkness & Wilson<br>1979                            | -     | 13.9±0.1  | 14.0               |

because it constituted a substantial topographic feature. This topographic confinement, in combination with the decoupling of the BIIS and FIS further north, resulted in the NSL advancing down the western margin only of the North Sea Basin to the north Norfolk coast where it emplaced the late stage tills. In this area of the southern North Sea, Dove *et al.* (2017) record a series of broad sedimentary wedges and associated moraines (sub-marginal till wedges) that document inset marginal locations of the NSL, classified as stillstand margins 1–4, and formerly regarded as the

Bolders Bank Formation (Jansen *et al.* 1979; Balson & Jeffrey 1991; Cameron *et al.* 1992). This represents a record of northerly retreat punctuated by readvances, indicative of an oscillating NSL margin. Margin 1 aligns with the onshore limit of the NSL, demarcated by the Garret Hill Moraine in north Norfolk (Pawley *et al.* 2006; Moorlock *et al.* 2008; Roberts *et al.* 2018; Evans *et al.* 2019) and Margin 2 appears to continue on land as the Hogsthorpe-Killingholme Moraine of the Lincolnshire Marsh (Straw 1979; Evans *et al.* 2019). Margins 3 and 4 are inset within Margin 2

and appear to arc northwards to align with the moraines on Holderness.

The impact of the NSL along the Durham and Northumberland coasts and its interaction with inland ice sources is evidenced by various features. Onshore multiple till sequences separated by glaciifluvial sediments record ice moving eastward into the North Sea from inland sources (e.g. the Tyne Ice stream) before being displaced by the southward-flowing NSL (Eyles *et al.*, 1982; Davies *et al.*, 2009; Livingstone *et al.*, 2015; Fig. 1). Just offshore, partially excavated, streamlined, mixed-bed terrain shows the NSL dominating the latter stages of the last glacial cycle, with ice streams such as the Tyne and Tweed either in recession or being deflected south (Everest *et al.* 2005; Livingstone *et al.*, 2010a; Roberts *et al.*, 2019). There is also a clear set of ice-contact, marginal landforms that document the initial decoupling of the NSL and inland ice (Staines 2009; Teasdale, 2013). Livingstone *et al.* (2015; cf. Davies *et al.* 2019) date this uncoupling at 18.5–18.3 ka based on surface exposure ages in the western Tyne Gap. The uncoupling also led to the development of several ice-dammed lakes along the Durham coast (e.g. glacial lakes Tees, Edder Acres and Wear).

Further north, the onshore regions adjacent to the Firth of Forth, Firth of Tay, Strathmore and the Moray Firth were dominated glaciologically by large ice streams during the last glacial cycle (Jamieson 1906; Linton 1959, 1962; Sissons 1963; Golledge and Stoker 2006; Hughes *et al.* 2010, 2014; Fig. 3). Many early workers identified an initial east/southeast ice flow across the Strathmore region sourced from the Grampian mountains, with a later switch in ice flow direction to the northeast along the Strathmore valley suggesting a more southerly source of ice or perhaps topographic influence on flow direction as the ice thinned (Bremner 1943; Charlesworth 1956; Synge 1956; Armstrong *et al.* 1985; Merritt *et al.* 2003). Golledge and Stoker (2006) assessed the subglacial bedform signature in the Strathmore area and concluded that the landforms represented a former ice stream (Strathmore Ice Stream), which was probably coalescent with a large ice stream in the Firth of Forth (Firth of Forth Ice Stream). Indeed, the geomorphology of the onshore corridors adjacent to the Firth of Forth (i.e. the Edinburgh and Kircaldy coasts) also exhibit streamlined bedforms in the form of streamlined bedrock bumps, crag and tails and drumlins, and these demonstrate ice broadly flowing east and bending southeast towards the Northumberland coast (Sissons 1971; Evans and Hansom 1996; Fig. 3). Additional evidence for ice streaming offshore was linked to deeply incised channels/tunnel valleys and seafloor glacial lineations running southwest–northeast from Montrose. Golledge and Stoker (2006) also suggested that the Wee Bankie Moraine complex may represent a shear margin moraine, although recent work suggests it is more likely to represent the onshore retreat of Firth of Forth ice during deglaciation (Roberts *et al.* 2019).

Following the work of Golledge and Stoker (2006), Hughes *et al.* (2010, 2014) constructed a comprehensive map of bedform types (e.g. drumlins, mega-scale glacial lineations, crag and tails) in this region and reconstructed complex changes in ice dynamics based on flowset mapping. This showed both the Strathmore Ice Stream and the Firth of Forth Ice Stream responding to changes in ice thickness, ice divide migration and topographic influences during the last glacial cycle, but clearly demonstrated that the Strathmore Ice Stream and Firth of Forth Ice Stream were key sources of ice heading northeast, east and southeast into the central North Sea. The behaviour of the Firth of Forth Ice Stream offshore is poorly understood during the build-up to the LGM, but advances have been made in understanding the role of Firth of Forth ice in controlling the NSL; indeed it is highly likely that the NSL was an offshore extension of the Firth of Forth Ice Stream. This

is supported by the imprint of the Bolders Bank Formation, subglacial bedforms, tunnel valleys and moraines on the seafloor as well as onshore stacked tills and ice margin geomorphology down the east coast of Britain and in the vicinity of Dogger Bank (Dove *et al.* 2017; Roberts *et al.* 2018; Emery *et al.* 2019), all of which supports previous work and demonstrates that Scottish ice was flowing from the Firth of Forth into the southern North Sea (Boulton *et al.* 1985; Davies *et al.* 2009; Evans and Thompson 2010; Busfield *et al.* 2015; Dove *et al.* 2017).

## Methods

### *Sampling and stratigraphy*

The sediments and stratigraphies of all locations (Figs 4–6) were analysed either from natural coastal cliff and quarried exposures in onshore settings or from seismic and bathymetric data and sediment cores in offshore settings. Sedimentological analysis followed a lithofacies approach with sediments classified on the basis of colour, particle size, clast lithologies and sedimentary structures (cf. Evans and Benn 2004), and observations and data were compiled on vertical profile logs and in some cases scaled photo mosaics. Detailed information included primary sedimentary structures, bed contacts, sediment body geometry, sorting and texture and secondary structures, as well as data on clast form and lithology and palaeocurrents where appropriate. Further details in terms of site-specific analyses are available in Evans *et al.* (2017, 2018, 2019), Bateman *et al.* (2018) and Roberts *et al.* (2018, 2019). The sediment–landform associations identified both onshore and offshore were placed in a glacial land-systems context established for the region by earlier research (Eyles *et al.* 1982; Evans *et al.* 1995; Bradwell *et al.* 2008; Davies *et al.* 2009; Boston *et al.* 2010; Evans & Thomson 2010; Roberts *et al.* 2013; Sejrup *et al.* 2015; Dove *et al.* 2017) as well as a regional lithostratigraphic context (cf. Straw 1979; Cameron *et al.* 1987, 1992; Balson & Jeffrey 1991; Eyles *et al.* 1994; Carr *et al.* 2006; Pawley *et al.* 2006; Catt 2007; Bateman *et al.* 2008; Sejrup *et al.* 2009; Davies *et al.* 2011).

### *Geochronology*

Geochronology was secured using a combination of OSL and radiocarbon dating (Table 1). All BRITICE-CHRONO OSL ages were based on extracted and cleaned quartz grains of 180–250 µm diameter, which were prepared under controlled light conditions as per Bateman and Catt (1996) and measured using an automated Risø luminescence reader. Equivalent dose ( $D_e$ ) estimates were measured unless stated otherwise using the SAR protocol of Murray and Wintle (2000, 2003) on small multigrain aliquots containing ~20 quartz grains each. Up to 80 small multigrain aliquots were measured for each sample in order to have a representative  $D_e$  dose distribution.

For the new Maiden Castle and Sandsend OSL ages presented as part of this paper (Table 2), measurements with the SAR protocol included an additional second recycling point, using IR stimulation prior to OSL measurement, in order to detect and exclude aliquots with any feldspar contamination. Within the SAR protocol, a preheat of 220 °C and 180 °C for 10 s was used to measure the samples from Maiden Castle and Sandsend, respectively. These temperatures were selected as the most appropriate, based on a dose recovery preheat temperature test performed on samples Shfd14068 (Maiden Castle) and Shfd13067 (Sendsend), which recovered to a given ratio consistent with unity.  $D_e$  values were accepted only if the relative uncertainty on the natural test–dose response was less than 20%, the recycling and the IR depletion ratio, including uncertainties, were within 20% of unity, and the recuperation

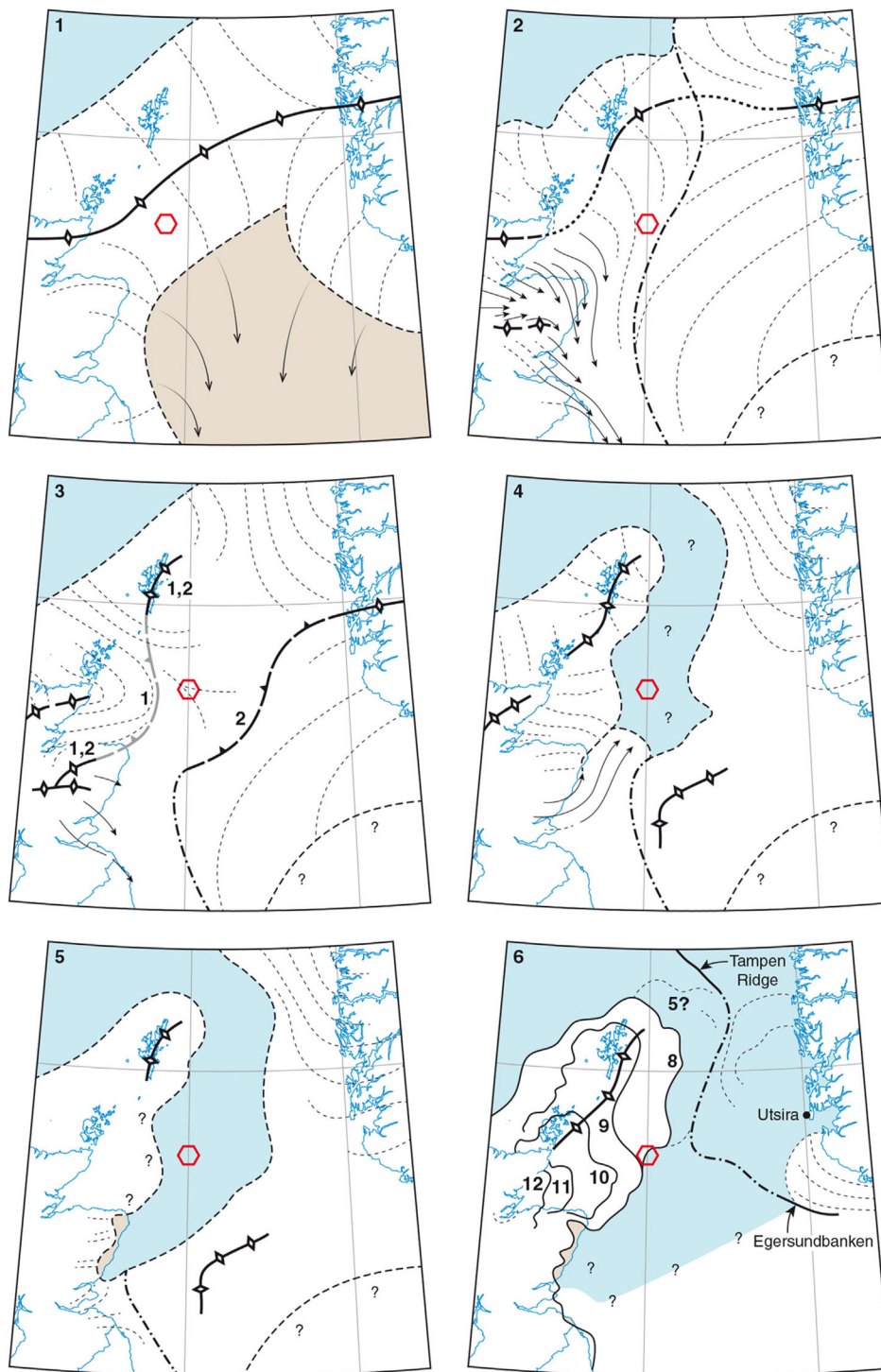


**Figure 3.** Palaeoglaciology of eastern Scottish coast and adjacent offshore area (from Merritt *et al.* 2017): 1) reconstruction of Boulton *et al.* (1985); 2) local LGM (stage 2); 3) considerable thinning and glacial reorganisation during stages 3 and 4; 4) re-expansion following initial marine ingress into Witch Ground Basin during stage 5, followed by probable coalescence of BIIS and the Norwegian Channel Ice Stream at the Tampen Ridge (see panel 6 for limits); 5) marine ingress into Lunan Bay during stage 7; 6) stages 8–12 and other limits (after Clark *et al.* 2012). Red hexagons show the centre of the Witch Ground Basin. Ice divides shown by thick black lines with open diamonds; single filled ticks denote ice divide receding by ice stream headward scavenging.

was less than 5%. These criteria lead to  $D_e$  distributions containing ~60 independent values per sample. These distributions are highly scattered, with a number of the independent values in the high dose region, indicating that these samples were affected by incomplete bleaching (i.e. insufficient exposure to daylight during transport to reset the luminescence signal). This is the case for all but sample Shfd14068, which is characterised by a normal distribution. In this latter case, the final  $D_e$  was estimated through the Central

Age Model (CAM, Galbraith *et al.* 1999). For the samples affected by incomplete bleaching, the internal–external uncertainty model (IEU, Thomsen *et al.*, 2007) has been applied in order to base the final  $D_e$  estimate on the dose population most likely to belong to well-bleached grains. To apply the IEU approach, an a-value of 0.2 and b-value of 1.5, as determined from a dose recovery test, have been used.

Total dose rates were calculated based on gamma contributions, measured using an EG&G MicroNomad gamma field

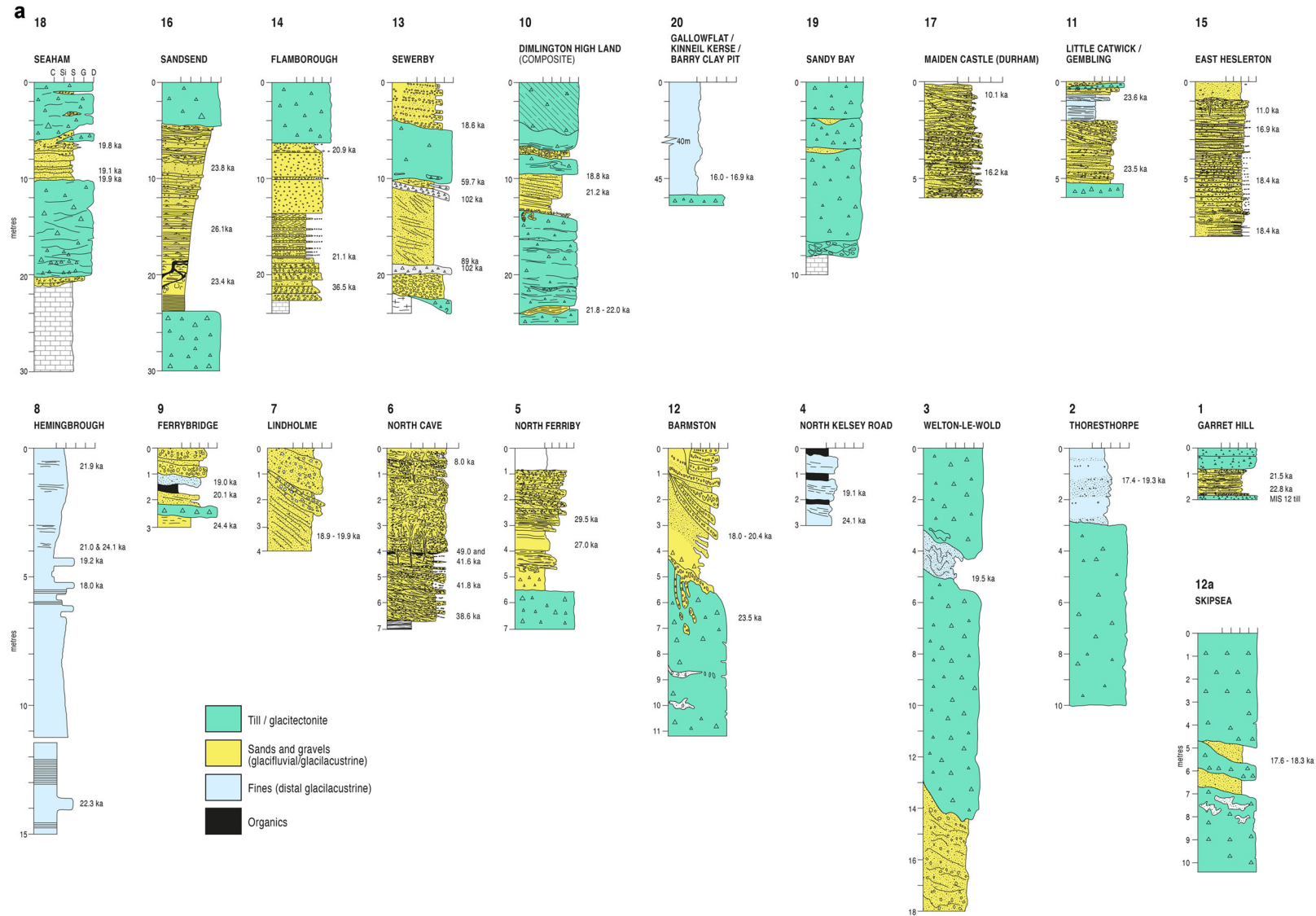


**Figure 4.** Vertical profile logs (from various sources) compiled at the locations critical to the palaeoglaciological reconstructions in this paper: a) onshore sites; b) and c) offshore core sites (green units are till/glaciectonite). For site locations see Fig. 1. Dates and date ranges are compiled from Table 1, with additional dates included for the onshore sites of Flamborough and Sewerby for broader context, as reported by Bateman *et al.* (2015).

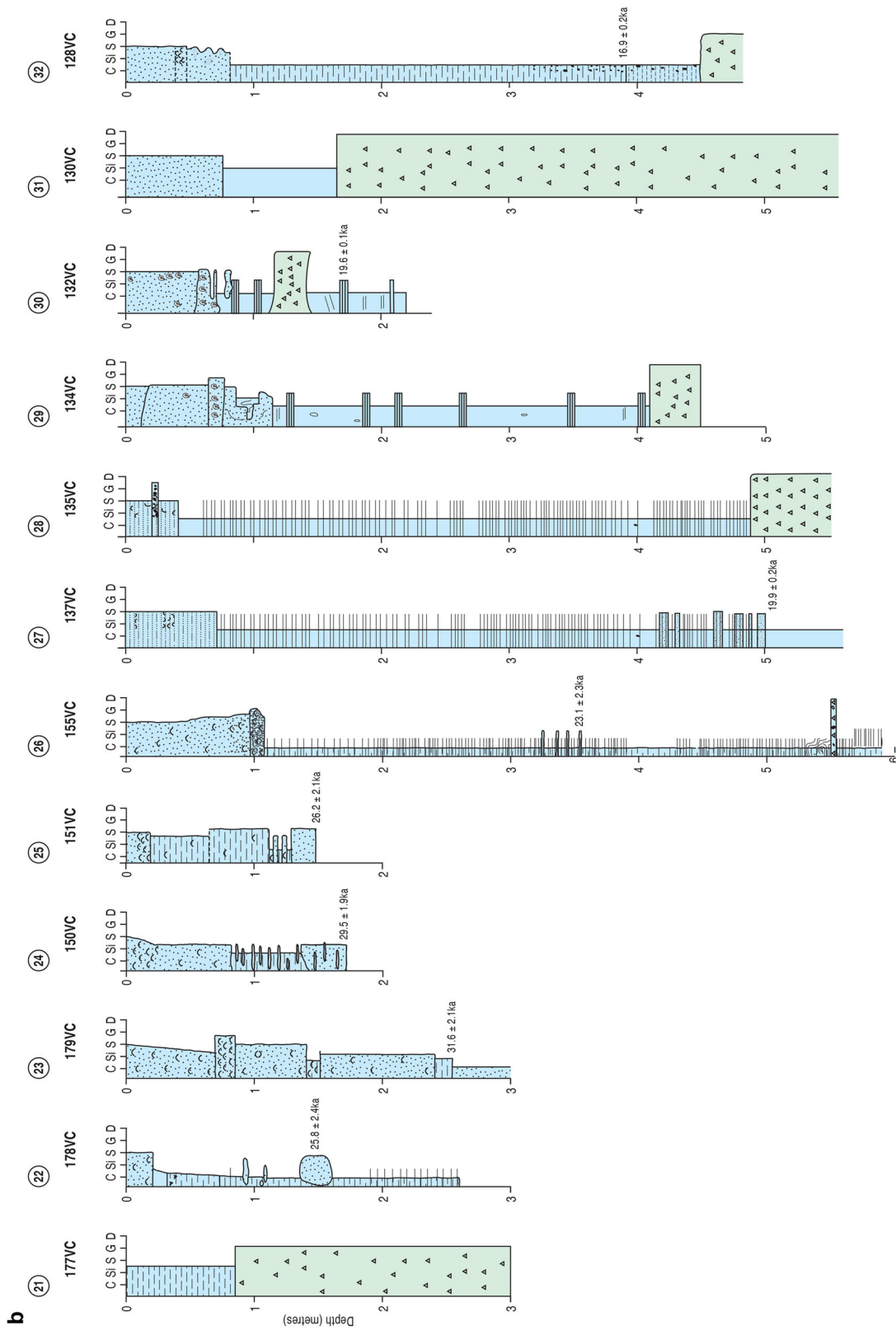


Figure 4. Continued

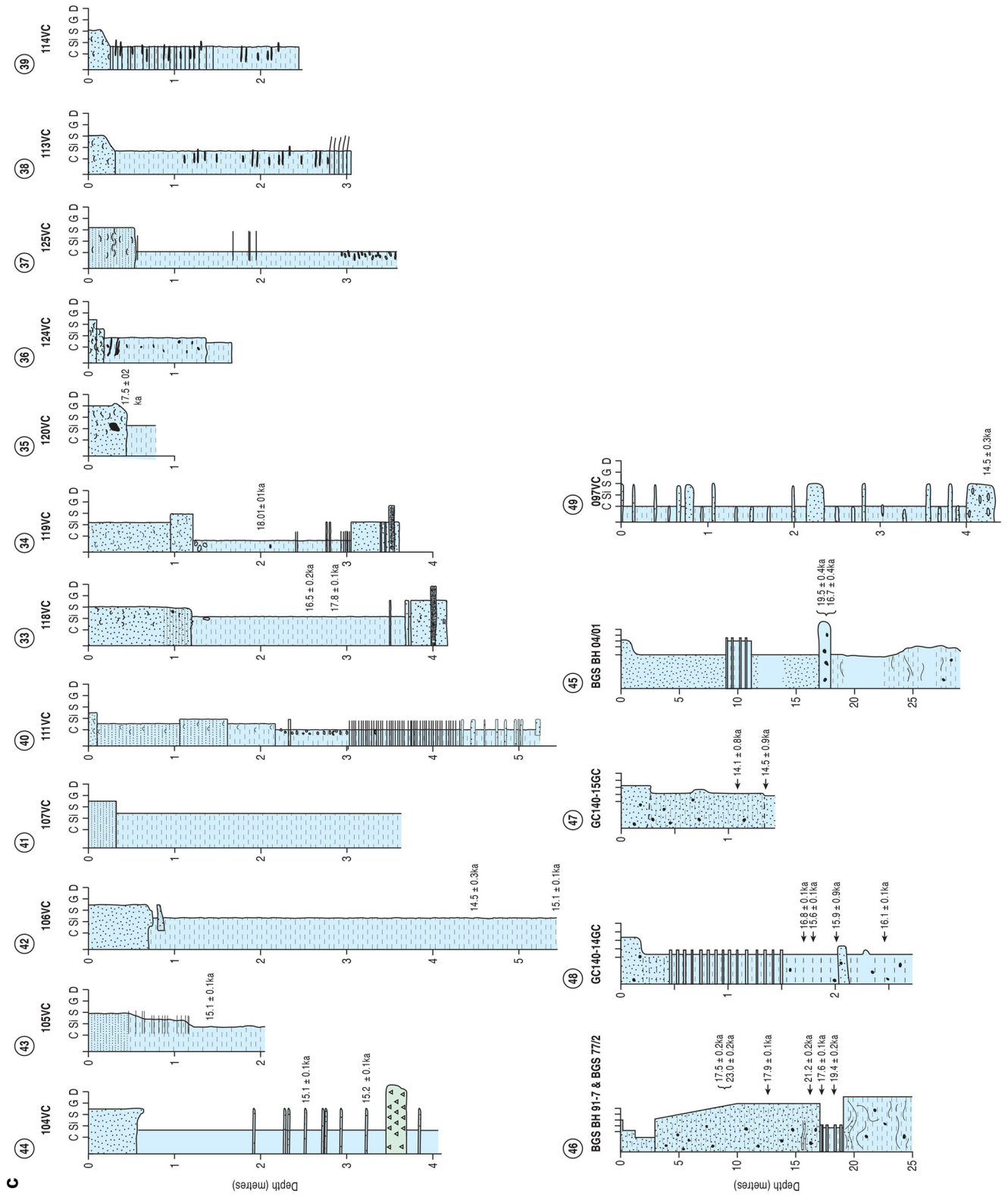
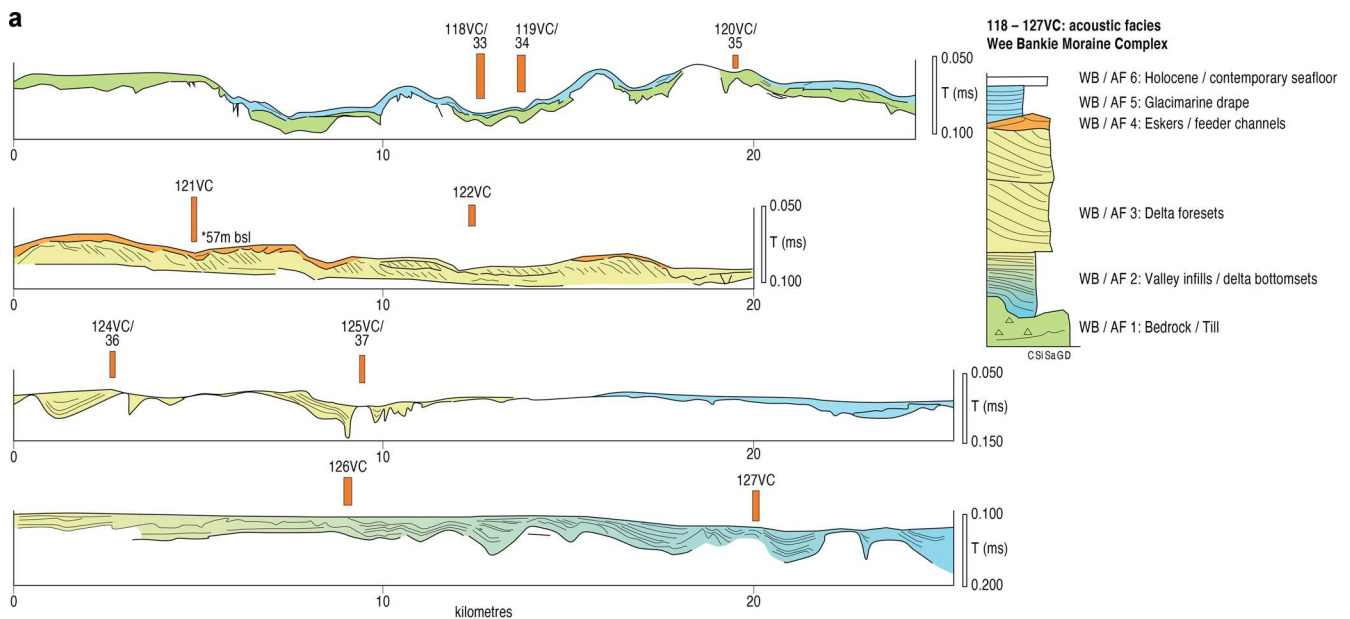


Figure 4. Continued



**Figure 5.** Offshore stratigraphic architecture and selected vertical profile logs based on acoustic and core data. Transect lines are located by blue dashed lines in Fig. 1: a) Acoustic stratigraphy to the east of Great Fisher Bank associated with core locations 112VC–114VC where the seafloor is marked by a distinctive scarp/step formed by glacitectonised lake sediments and a subaqueous ice-contact fan; hence, this may mark a former ice margin; b) Between core locations 111VC and 104VC the seafloor displays a series of subglacial tills draped by glacimarine sediments with inset moraines marking grounding line retreat towards Bosies Bank between 17.5 and 15.0 cal. ka BP; c) Between core locations 127VC and 118VC an east-to-west acoustic profile shows deglacial glacimarine sediments transitioning to shallower ice-marginal delta complexes as the ice sheet retreated west into the Firth of Forth. The Wee Bankie Moraine complex is thus composed of both drowned deltas to the east as well as push moraines to the west. Cores 118VC–120VC provide deglacial ages for the Wee Bankie Moraine complex of 18.0 to 16.5 cal. ka BP.

spectrometer and beta contributions based on elemental analysis using inductively coupled plasma mass spectroscopy (ICP-MS) at SGS laboratories Ontario, Canada. The dose rates from radionuclide concentrations were derived from the conversion factors of Guérin *et al.* (2011). A linear accumulation of deposits has been assumed in order to calculate the contribution of cosmic radiation according to a varying burial depth (based on Prescott and Hutton, 1994). Finally, the total dose rates as shown in Table 2 were calculated according to attenuation caused by moisture and grain size.  $D_e$  estimates and further details associated with the OSL ages from Maiden Castle and Sandsend are presented in the Supplementary Information.

Accurately determining the average palaeo-moisture since burial has proved challenging, as groundwater levels through time have changed markedly for most samples due to ice and permafrost degradation, sea-level changes and formation and emptying of proglacial lakes. Hence, present-day moisture levels are thought unlikely to reflect average palaeo-moisture levels. Consequently, sites and samples were evaluated based on whether evidence suggested they had been saturated for most or a substantial part of their burial history in which case palaeo-moisture values of 27% and 23% were applied, respectively. If samples were only partially saturated or minimally saturated during burial, values of 15% or 10% were applied, respectively. To cover fluctuations, wide uncertainties of  $\pm 5\%$  on all water content were adopted to include variations related to porosity and compaction. For consistency, these four possible palaeo-moisture values were applied to all BRITICE-CHRONO OSL samples. For example, samples at Garret Hill, Norfolk (Shfd15033 and Shfd15034), at 9 m OD and in glacial sands underlain by free-draining chalk, were assigned palaeo-moisture values of 10%. In contrast, samples from Thoresthorpe, Lincolnshire (Shfd15154

and Shfd15155), at 12 m OD and in ice-marginal lacustrine sediments, which even today have a perched near-surface groundwater table, were assigned saturated moisture values of 27%. Of particular note were samples collected from eroded shore-line cliff sections in sand units between diamictos. Initially many of these were assessed as minimally saturated (10%) or partially saturated (20%). However, re-evaluation has established that prior to cliff erosion such intercalated sands within diamictos would have acted either as aquifers or have been below the groundwater table. High regional water tables are evidenced by the ongoing presence of Hornsea Mere, found in a topographic low on the diamicton. As a result, palaeo-moisture values have been adjusted and in many cases increased. Moreover, previously published ages have been recalculated to better reflect what is believed to be true palaeo-moisture levels (see Table S1) and to be consistent with the regional OSL age dataset (Table 1). For full details of OSL measurement protocols, approaches to  $D_e$  data analysis, age estimation and associated details, readers should consult the source publication where they were originally published as shown in Table 1.

As a result of the above revisions, the model proposed by Bateman *et al.* (2018) of initial NSL incursion into the Humber Gap at 21.6 ka (Stage 1) is revised to  $\sim 29$  ka and its retreat offshore from the present terrestrial record, originally dated at  $\sim 18$  ka (Stage 2), is revised to  $\sim 20$  ka. Impoundment of Lake Humber occurred at least by 24 ka until 18 ka with Lake Pickering being at least partially coeval with this. Full withdrawal of the NSL from the Yorkshire region occurred prior to  $\sim 19$  ka (previously  $\sim 15$  ka; Stage 4 of Bateman *et al.* 2018).

Radiocarbon dates were obtained from a mixture of paired bivalves, mixed benthic foraminifera samples and shell fragments. The shell fragments and bivalves were cleaned with deionised water and dried at 40 °C in an oven.

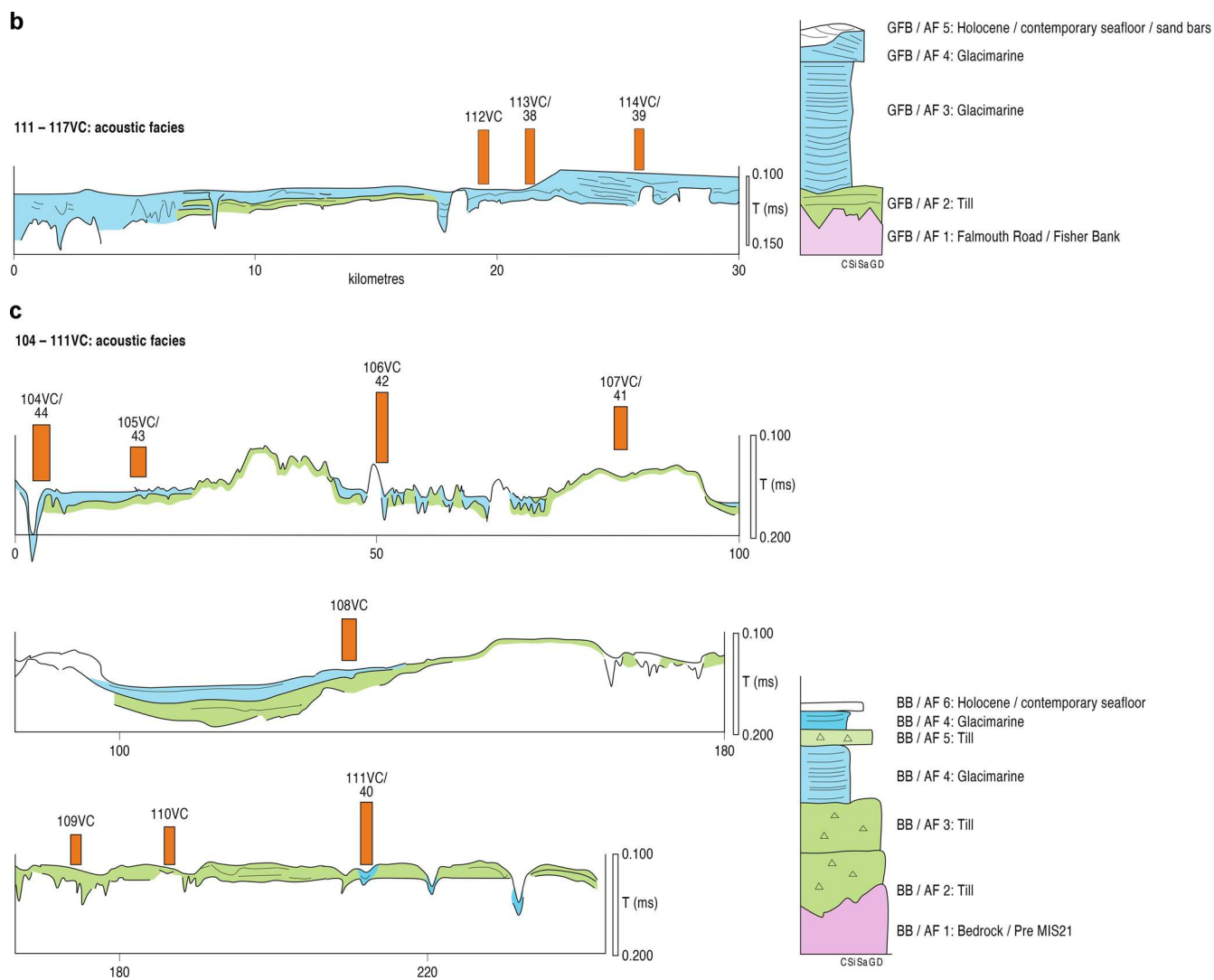


Figure 5. Continued

Foraminifera were sieved through 500  $\mu\text{m}$ , 180  $\mu\text{m}$  and 63  $\mu\text{m}$  sieves and dried at 40  $^{\circ}\text{C}$  and then whole, unabraded specimens were picked dry from the 500–180  $\mu\text{m}$  fraction. Conventional ages were calibrated using the Marine13 curve with an inbuilt marine reservoir correction of 400 years and a  $\Delta R$  of 0 years (Calib v7.0 software; Reimer *et al.*, 2013) and reported here as the calibrated 1 $\sigma$  median result. Importantly, it is likely that samples would be subject to large and variable local  $\Delta R$  during the LGM and the Lateglacial period.

A number of previously reported legacy dates were available to augment the chronology established by BRITICE-CHRONO Transect 2 (Table 1). These are integrated into the various sections below where pertinent and used alongside the BRITICE-CHRONO dates in order to compile a regional reconstruction of ice-sheet dynamics in the North Sea region.

The glacial geomorphology and stratigraphy of the North Sea and eastern England have been used to define seven distinctive former ice-sheet limits (Fig. 6). This deglaciation sequence provides a prior model (i.e. the hypothetical ‘relative order’ of events) for Bayesian statistical analysis of the independent dating of these sediments (e.g. Chiverrell *et al.* 2013). The complexity of the region necessitates dividing the glacial retreat sequence and geochronology into two models describing first a southern sequence, from Norfolk to

the Firth of Forth, and second a northern sequence, from the Fladen Moraines to the Moray Firth. Both Bayesian prior models were developed independently and included all geochronology (Bronk Ramsey 2008, 2009a, b; Bronk Ramsey and Lee 2013). These two prior models were determined independently of the geochronological data and here constitute the net ice-marginal pattern of retreat integrating small-scale readvances and stillstands. The Bayesian modelling used uniform phase sequence models that were punctuated by boundaries and were coded using OxCal 4.3 (Bronk Ramsey and Lee 2013). The statistical analyses use Markov Chain Monte Carlo sampling to build up a distribution of possible solutions, generating probabilities called posterior density estimates, and these are the product of both the prior or relative-order model and the likelihood (measured age) probabilities for each sample. Each retreat zone was coded in the models as Phases, containing grouped dating information for sites that shared a common relationship with the preceding and subsequent zones. Phases were separated by the Boundary command and generated a modelled age probability distribution output for the major ice limits.

Both sequence models were run in outlier mode in order to assess outliers in time using a Student’s *t*-distribution ( $P < 0.05$ ) to describe the outlier distribution and a scaling of  $10^0$ – $10^4$  years (Bronk Ramsey, 2009b). The models were run initially to

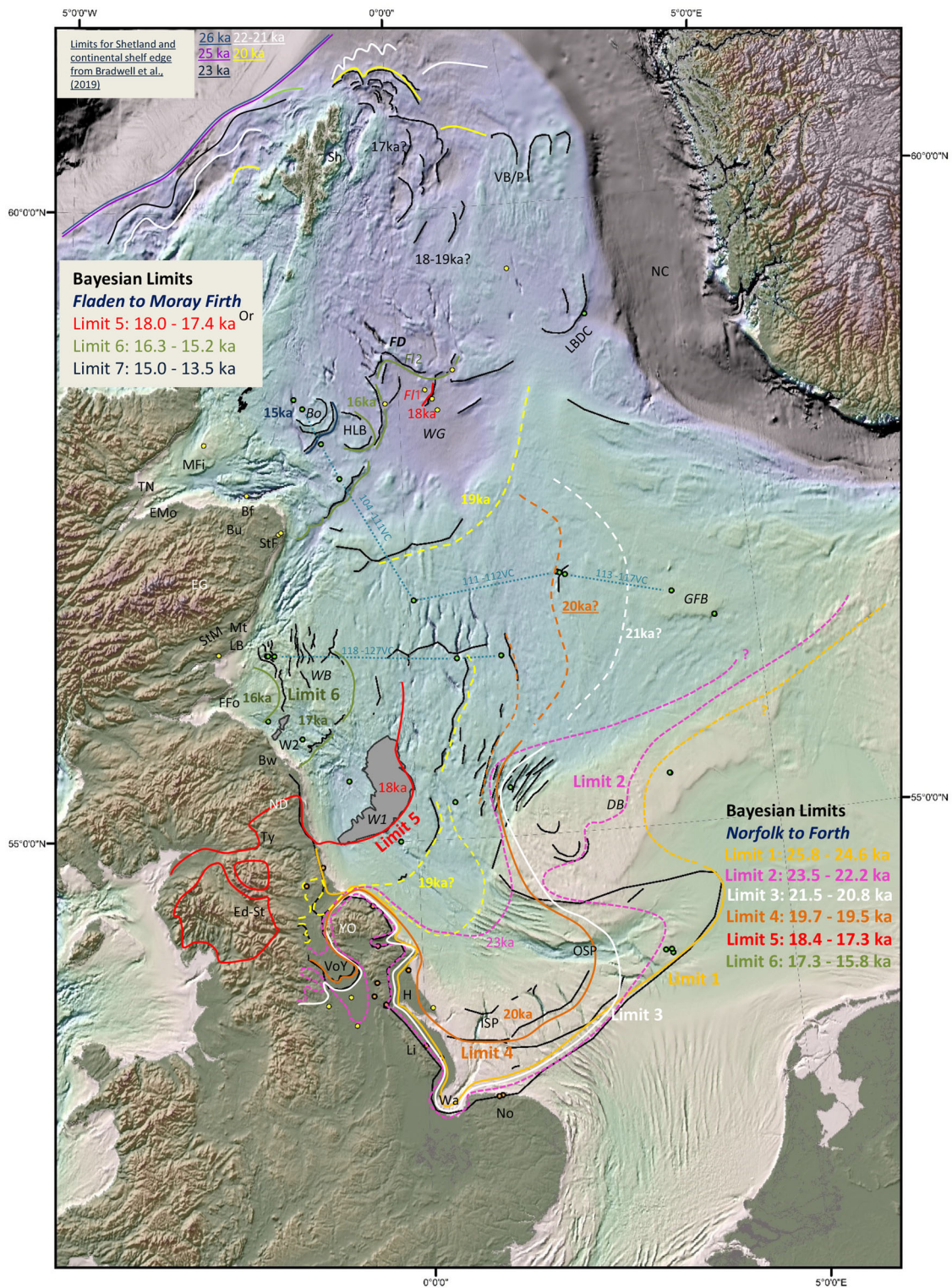


**Figure 6.** Bathymetry and topography of the North Sea region, showing ice-sheet advance and retreat patterns for the period 25.8–13.5 ka with ice limits determined by Bayesian analysis. Black lines demarcate major moraines and/or till limits. The main Bayesian Limits 1–7 are anchored by major moraine or grounding zone wedge complexes (grey coloured areas W1 and W2 are grounding zone wedges). Morphostratigraphic controls clearly show that Limits 2, 3, 4 and 5 are associated with regional readvances between ~24 and 18 ka. The Limit 4 to Limit 5 marks a transition between glacialterrestrial and glacialmarine conditions in the southern and central North Sea. In the northern North Sea deglacial isochrones for Shetland and the continental shelf edge are sourced from Bradwell *et al.* (2019), also derived using Bayesian modelling.

give obvious outliers a probability scaling of  $P=1$  and using a high generic probability of all other ages being outliers ( $P<0.2$ ). This process identified a series of statistical outlier ages. These outliers were not disregarded automatically, but explanations were sought in terms of stratigraphical context or geochronological measurement (e.g. poor resetting of the OSL signal). Subsequent iterative runs of the Bayesian modelling

gradually reduced the individual outlier probabilities, with  $P<0.1$ ,  $P>0.2$ ,  $P>0.5$  and  $P>0.95$  reflecting an increasing order of outlier severity. Ultimately, the Bayesian analyses produced conformable age models, with overall model agreement indices of 179% (Norfolk to Firth of Forth) and 132% (Fladen to Moray), both exceeding the >60% threshold advocated by Bronk Ramsey (2009a). Agreement indices were

**Table 2.** Summary of previously unreported OSL estimated ages and associated information for three samples from Sandsend (North Yorkshire) and two samples from Maiden Castle (County Durham). Depth, water content and the calculated contribution to the total dose rates are summarised. The table also includes information on the total number of aliquots measured with OSL which passed the acceptance criteria and the overdispersion (OD) of the resulting dose distribution. Reported equivalent doses ( $D_e$ ) for all samples except Shfd14068 were derived using the IEU approach. The exception (Shfd14068) involved the application of the CAM instead of IEU, as the  $D_e$  population was normally distributed and therefore not affected by incomplete bleaching.

| Lab code             | Depth (m) | w (%) | $\beta$ dose rate (Gy/ka) | $\gamma$ dose rate (Gy/ka) | Cosmic dose rate (Gy/ka) | Total dose rate (Gy/ka) | Aliquots accepted (measured) | OD (%) | Equivalent dose (Gy) | Age (ka)   |
|----------------------|-----------|-------|---------------------------|----------------------------|--------------------------|-------------------------|------------------------------|--------|----------------------|------------|
| <b>Sandsend</b>      | Shfd13066 | 21.8  | 0.66 ± 0.06               | 0.57 ± 0.04                | 0.03 ± 0.001             | 1.27 ± 0.07             | 29 (29)                      | 55     | 30.1 ± 1.7           | 23.8 ± 1.8 |
|                      | Shfd13067 | 16.8  | 0.67 ± 0.05               | 0.56 ± 0.04                | 0.04 ± 0.002             | 1.28 ± 0.007            | 31 (94)                      | 54     | 33.5 ± 2.1           | 26.1 ± 2.1 |
|                      | Shfd13068 | 12.0  | 0.47 ± 0.04               | 0.56 ± 0.04                | 0.05 ± 0.003             | 1.10 ± 0.05             | 28 (73)                      | 63     | 25.9 ± 1.4           | 23.4 ± 1.7 |
| <b>Maiden Castle</b> | Shfd14067 | 2.7   | 0.52 ± 0.04               | 0.46 ± 0.03                | 0.13 ± 0.006             | 1.16 ± 0.05             | 39 (98)                      | 91     | 18.7 ± 2.7           | 16.2 ± 0.8 |
|                      | Shfd14068 | 1.0   | 0.57 ± 0.04               | 0.60 ± 0.03                | 0.18 ± 0.009             | 1.32 ± 0.05             | 34 (98)                      | 46     | 13.3 ± 1.2           | 10.1 ± 1.0 |

calculated for individual age determinations, identifying samples that did not agree with the model; individual agreement indices should usually be over 60%. The Bayesian modelling has generated modelled ages for boundaries between seven ice limits (L1–7) related to ice advance and retreat from Norfolk into the Firth of Forth and also further north into the Moray Firth (Figs 6 and 7).

## Glacial geomorphology and chronological controls

### Southern sector

#### Defining and dating pre-LGM ice extent

Evidence of terrestrial environmental conditions immediately prior to MIS 2 is contained within fluvio-periglacial fan deposits on the east side of the Glacial Lake Humber basin (North Cave, Fig. 4a; Evans *et al.* 2018). The earliest of these deposits date to MIS 3, based on OSL ages of 38.6–41.8 ka (Shfd 13058 and Shfd 13059) and radiocarbon ages of 41.6–49.0 ka (SUERC-77600 and SUERC79023; Table 1). Importantly, the fan deposits were prograded to near or below 0 m OD and hence indicate that Glacial Lake Humber did not occupy the area until later, during MIS 2, at which time the lake waters only reached 8 m OD. The basal pair of ages from North Cave constrains ice-free conditions in the region prior to ice advance and predates the MIS 2 ice advance by an unknown period. The coding in the Bayesian analysis uses an “After” constraint for these ages, which focuses the modelling towards the subsequent chronology that directly dates proglacial settings associated with the Limit 1 NSL advance.

The southernmost extent of MIS 2 glaciation in eastern England has traditionally been associated with the outer edge of the Skipsea Till in Holderness (Catt & Penny 1966; Catt 2007), the Upper Marsh Till in Lincolnshire (Straw 1957, 1958, 1961, 1979) and the Hunstanton Till (Holkham Member, Lewis 1999) in north Norfolk (Suggate & West 1959; Straw 1960, 1979), all of which are lithostratigraphically equivalent (Boston *et al.* 2010). Moraines associated with this limit are not particularly widespread but are developed instead immediately inboard of the till limits; for example, the Holderness hummocky drift, extending from Gembling in the north to Catwick and then to Mill Hill in the south, (Eyles *et al.* 1994; Evans & Thomson 2010) and the Hogsthorpe–Killingholme Moraine of the Lincolnshire Marsh (Straw 1979), both of which have been explained as readvance positions. Additionally, the Horkstow Moraine in the Humber Estuary and the Stickney Moraine and Hunstanton Till (Holkham Member) in The Wash have been equated with an early Devensian (MIS 3/4) glaciation by Straw (1979) and related to his Lower Marsh Till. However, Evans *et al.* (2019) have pointed out that the Lower and Upper Marsh Tills have never been observed together in a single exposure and early depictions of the last glaciation limit are drawn at the more extensive, Lower Marsh Till position (e.g. Clayton 1957). Therefore, Evans *et al.* (2019) propose that the Stickney and Horkstow moraines represent the MIS 2 limit, in agreement with the age determination of Bateman *et al.* (2018). On the north Norfolk coast, the Garret Hill Moraine (Pawley *et al.* 2006) is associated with the Hunstanton Till limit and hence regarded as MIS 2 in age (Evans *et al.* 2019; Roberts *et al.*, 2019).

#### Limit 1 – NSL advance (pre-31–25 ka)

The nature of the glacial landforms of the southern North Sea have recently been reported by Dove *et al.* (2017) and dated by Roberts *et al.* (2018). The most extensive MIS 2 limit (Limit

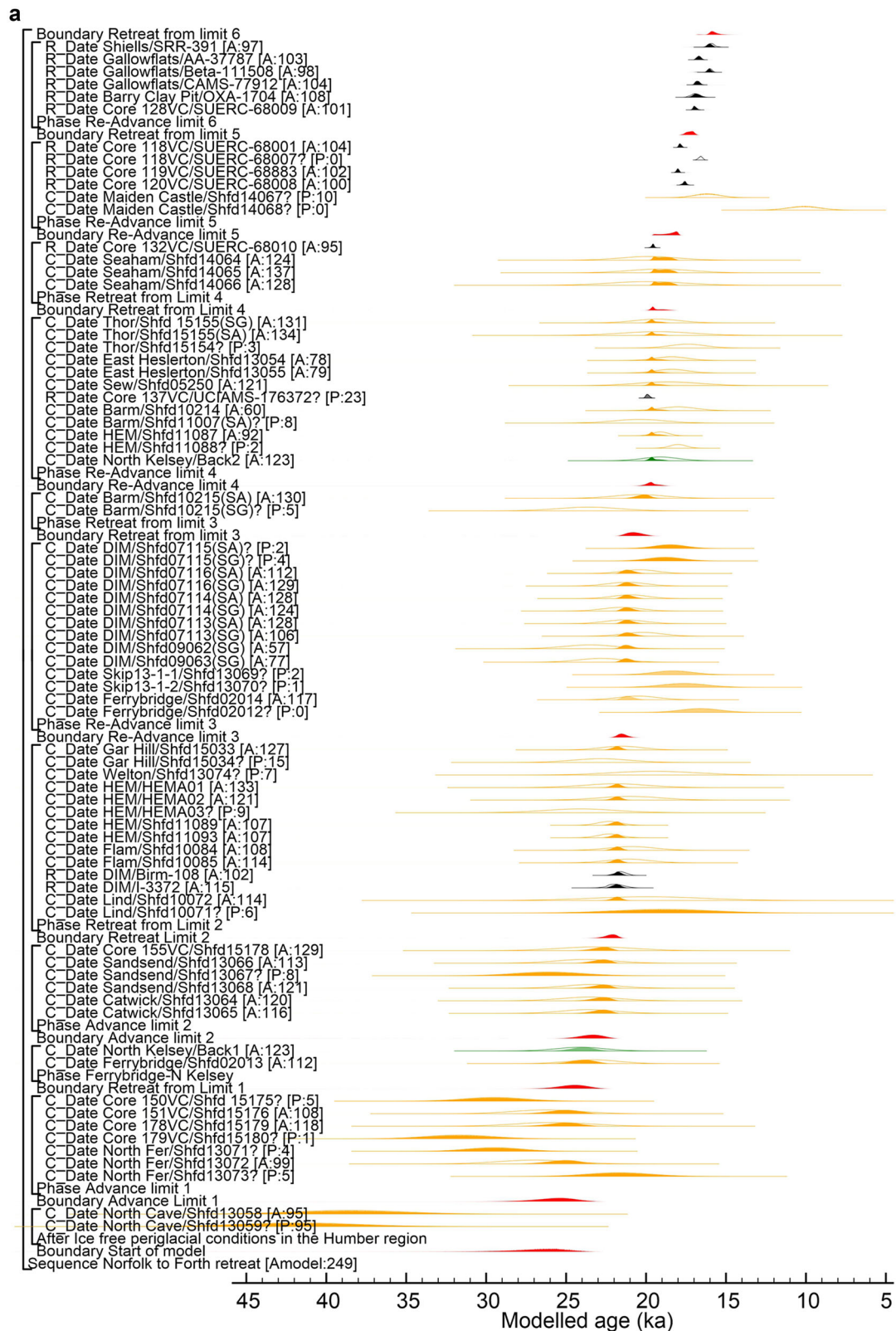


**Figure 7.** Bayesian models for the dating of ice retreat from (a) Norfolk to the Firth of Forth and (b) the Fladen 1 Moraine to the Moray Firth. The model structure shown uses OxCal brackets (left) and keywords that define the relative order of events (Bronk Ramsey, 2009a, b). Each original distribution (open symbol) represents the relative probability of each age estimate with posterior density estimate (solid symbol) generated by the modelling. Shown are  $^{14}\text{C}$  ages (black/grey), luminescence ages (orange) and boundary ages produced in the modelling (Red). Outliers are denoted by their probability (e.g. [P:5]) of being an outlier indicated by low values  $<5$  (95% confidence). Overall model agreement indices (e.g. [Amodel:100]) are shown alongside the agreement indices for individual ages (e.g. [A:66]), identifying their fit to the model ( $>60\%$  is the widely used agreement threshold for 'good' fit (Bronk Ramsey, 2009a, b)).

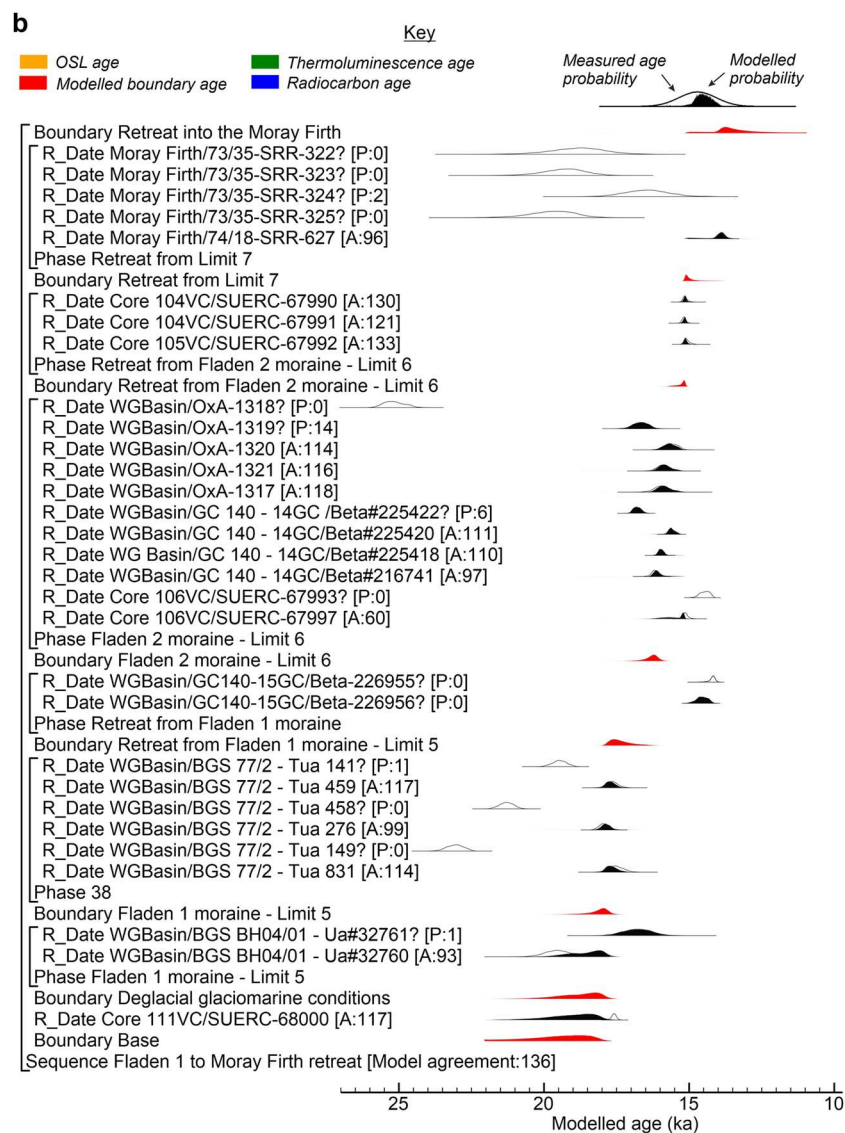


**Figure 7.** Continued

1) is recorded by till at the base of cores 138–141VC and 177VC and dated to 29–30 ka in cores 178VC and 179VC, all located south of Dogger Bank (Roberts *et al.*, 2018; Table 1; Figs 1 and 4b). The glacialustrine sediments of the Dogger Bank date the Dogger Lake to 31.7–25.8 ka (Shfd15175, Shfd15176, Shfd15179, Shfd15180, Table 1). The western end of the lake was glacially overridden by ice that extended to ~54°N, co-incident with the southern limit of the Bolders Bank Formation (subglacial till). The overriding of the glacialustrine deposits resulted in compressive glacitectonism to form the Dogger Bank. This phase of overriding and subsequent northwards recession appears to have been rapid, being complete by  $23.1 \pm 2.3$  ka (Shfd15178, Table 1), and resulted in the construction of moraine complexes and ice-marginal deposits on both the southern and northern edges of the newly formed Dogger Bank. Retreat from Limit 1 is recorded by outwash over till in cores 178VC and 179VC, lake sediments in cores 150VC and 151VC (Roberts *et al.* 2018), and glacialustrine sediments and outwash on the proximal side of the North Ferriby moraine (Fig. 4a; Bateman *et al.* 2018). The Bayesian analysis identifies OSL age Shfd13073 as too young relative to subsequent locations in the model, and the remaining six ages divide into two clusters: an older group (Shfd13071, Shfd15180 and Shfd15175) is centred on

29–30 ka and a younger group (Shfd13072, Shfd15176 and Shfd15179) centred on 26–27 ka. The contexts for the two groups intermix within sequences and, given the potential for poor resetting of the OSL signal in proglacial outwash, the younger group is the more likely to be valid. This produced good agreement (>60%) in the model with the other four ages treated as complete outliers ( $P=1$ ) (Shfd13071/N Ferriby, Shfd15175 and Shfd15180/Dogger Bank), and constrains the advance to Limit 1 as  $post-25.8 \pm 1.4$  ka and  $pre-24.6 \pm 1.0$  ka (Fig. 7a). Assessing the influence of imposing the “After” constraint on the North Cave ages (Fig. 7a) was explored by coding those ages instead as a Phase, which also produced a conformable model (not shown) and constrains the Limit 1 advance to  $post-28.1 \pm 2.0$  ka and  $pre-25.0 \pm 1.1$  ka. The parsimonious interpretation is that ice advance into the region occurred after  $28.1 \pm 2.0$  ka, reaching the maximum regional extent at  $25.8 \pm 1.4$  ka to  $24.6 \pm 1.0$  ka.

#### *Limit 2 – NSL oscillation (~26–24 ka) and retreat (~22 ka)*

A subsequent advance to Limit 2 at 24–26 ka is evidenced by a buried moraine beneath the seafloor at core site 142VC and till patches over Dogger Bank (LF DB4b of Roberts *et al.* 2018). Onshore, the equivalent evidence for this advance is the lower

tills at Sandsend (Roberts *et al.* 2013) and Little Catwick/Gembling (Bateman *et al.* 2018; Fig. 4a). At Sandsend, OSL ages of  $23.8 \pm 1.8$  ka and  $23.4 \pm 1.7$  ka (Shfd13066 and Shfd13068; Table 1) date the uppermost sand and gravel outwash in a deglacial coarsening-upward lacustrine-to-fluvial sequence and thereby provide a minimum date on the underlying till. The Little Catwick/Gembling stratigraphy is typical of the advance and retreat/readvance Skipsea Till sequence identified by Evans and Thomson (2010) using regional stratigraphic reconstructions, with the lower till at the site appearing at a more advanced marginal position of the NSL than that preserved in the sediments at Flamborough, Barmston and Dimlington. At Little Catwick/Gembling and other sites further north, subaqueous fans and lake rhythmites deposited into a northern arm of Lake Humber were deposited over Skipsea Till at  $23.5 \pm 1.8$  ka and  $23.6 \pm 1.7$  ka (Shfd13064 and Shfd13065; revised from 22.8–23.4 ka in Bateman *et al.* 2018; Table 1). This advance also appears to equate with the earliest impoundment of Glacial Lake Humber, dated at  $24.1 \pm 1.5$  ka (Bateman *et al.* 2000; revised from  $22.7 \pm 1.4$  ka) using thermoluminescence (TL) at North Kelsey Road, Caistor (Fig. 4a; Back 1; Table 1) and  $24.4 \pm 1.6$  ka (Bateman *et al.* 2008; revised from  $23.3 \pm 1.5$  ka) using OSL of sub-till silts at Ferrybridge (Fig. 4a; Shfd02013; Table 1).

Retreat from Limit 2 appears to have taken place at around 23 ka and is constrained offshore by glacial lacustrine sediments that on-lap recessional moraines along the northern edge of Dogger Bank. These sediments show no evidence of subsequent glacial overriding and are OSL-dated in core 155VC to  $23.1 \pm 2.3$  ka (Shfd15178; Table 1). Onshore, this ice recession is constrained chronologically by the deglacial outwash between tills at Sandsend dated to  $23.4 \pm 1.7$  ka and  $23.8 \pm 1.8$  ka and at Catwick/Gembling dated to  $\sim 23.5$  ka (see above; Fig. 4a). The advance and retreat phase boundaries for Limit 2 from the Bayesian model are dated 23.5 and 22.2 ka, respectively (Fig. 7a).

#### Limit 3 – NSL advance ( $\sim 21.5$ ka) and subsequent retreat

A significant readvance to Limit 3 and subsequent retreat are recorded to the west and southwest of Dogger Bank and relate to the NSL flowing between Dogger Bank and the Yorkshire/Lincolnshire coasts down to north Norfolk, where the Garret Hill Moraine was constructed onshore. Here a maximum age on the emplacement of the Hunstanton Till (Holkham Member) and the associated Garret Hill Moraine (Pawley *et al.* 2006) is reported by Roberts *et al.* (2018) and Evans *et al.* (2019) at  $21.5 \pm 1.3$  ka (Shfd15033; Table 1) from glaciectonised glacial outwash overlying MIS 12 till (Fig. 4a). The outwash dates to  $22.8 \pm 1.8$  ka (Shfd15034; Table 1) and dates the attainment of Limit 3 by the NSL in this area. Retreat from Limit 3 is marked offshore of north Norfolk and Lincolnshire, by a series of superimposed, lobate-shaped till wedges that post-date the initial phases of the emplacement of the Bolders Bank Formation (Dove *et al.* 2017). These demonstrate that the NSL underwent a series of quasi-stable oscillations during recession.

Further north, in Lincolnshire, an OSL age of  $19.5 \pm 2.6$  ka (Shfd13074; Table 1) on glaciectonised ice-dammed lake sediments from beneath the Marsh Till at Welton-le-Wold (Fig. 4a) provides a maximum age on the advance to the Stickney and Horkstow moraines. In Yorkshire, this event is recorded by the emplacement of the Skipsea Till over the organics at Dimlington (Fig. 4a), radiocarbon-dated by Penny *et al.* (1969) at 22 cal ka BP (Birm-108 and I-3372; Table 1) and OSL-dated to  $23.5 \pm 1.6$  ka and  $22.8 \pm 1.4$  ka (Shfd09062 and Shfd09063; revised from 21.2 and 20.5 ka in Bateman

*et al.* 2015; Table 1), and at Flamborough Head (Fig. 4a) by sub-till sands that were OSL-dated by Bateman *et al.* (2015) and now have revised ages of  $20.9 \pm 1.4$  ka and  $21.1 \pm 1.3$  ka (Shfd10084, Shfd10085; Table 1). Dates recording the continued existence of Glacial Lake Humber at this time (Table 1) have been reported from Hemingbrough (Fig. 4a) and range from  $24.1 \pm 2.2$  ka to  $21.0 \pm 1.9$  ka (HEMA01-HEMA03; Table 1), although HEMA03 at 24.1 ka shows as a clear outlier (Fig. 7a).

At Lindholme (Fig. 2), Bateman *et al.* (2015) report ages of 18.2 ka and 19.1 ka (Shfd10071 and Shfd10072; revised here to  $18.9 \pm 3.0$  ka and  $19.9 \pm 3.4$  ka; Table 1) on glacial outwash sands in the vicinity of the proposed ice limit at Wroot (Fig. 4a). This appears to be the short-lived maximal limit of an ice lobe that extended down the Vale of York (Friend *et al.* 2016; Fig. 12 of Bateman *et al.* 2018). More prolonged stillstands are recognised by the extensive moraines at Escrick and York.

The age of retreat from Limit 3 is further documented at Dimlington on Holderness, in relation to inter-till stratified deposits, and at Hemingbrough in relation to Glacial Lake Humber deposits. A range of ages from 18.5 to 22.8 ka (Shfd07113-Shfd07115 and Shfd09062-Shfd09063; Table 1) on sands between the traditionally classified Skipsea and Withernsea tills at Dimlington (Catt & Penny 1966; Rose 1985; Boston *et al.* 2010; Evans & Thomson 2010; Fig. 4a) provide a chronological control on NSL recession from the East Yorkshire coast and the sedimentation of ice-contact to proglacial subaqueous fans and proximal bottomsets (LFA 2 of Evans & Thomson 2010). At Hemingbrough (Fig. 4a), OSL ages of  $19.2 \pm 0.5$  and  $18.0 \pm 0.6$  (Shfd11087 and Shfd11088; revised from the 16.8 and 15.5 of Bateman *et al.* 2015; Table 1) indicate that Glacial Lake Humber still existed at this time (NB. Shfd11088 is an outlier in the Bayesian analysis; Fig. 7a) and hence the Humber Estuary remained blocked even though the Holderness ice margin had receded enough to allow the development of an extensive lake to the north; this is therefore most likely a northern arm of Lake Humber (Fig. 12 of Bateman *et al.* 2018). The advance and retreat phase boundaries for Limit 3 from the Bayesian model are dated 21.5 and 20.8 ka, respectively (Fig. 7a).

#### Limits 4 and 5 – NSL oscillations and retreat ( $\sim 20$ – $17.2$ ka)

A long-recognised minor readvance on the East Yorkshire coast is defined here as Limit 4 and is demarcated by the emplacement of the Withernsea Till in the area around Dimlington (Catt & Penny 1966; Rose 1985; Evans & Thomson 2010). Although this readvance has traditionally been emphasised because it is stratigraphically documented by the Withernsea Till, it is only one of a number of potential onshore readvances (oscillations) by the margin of the NSL recorded in interbedded sequences of tills and ice-contact lake deposits on Holderness (Boston *et al.* 2010; Evans & Thomson 2010). Moreover, Boston *et al.* (2010) indicate that the Withernsea Till is lithologically internally complex and cannot be unequivocally differentiated geochemically from the equally complex Skipsea Till. Hence the same readvance could be recorded north of Dimlington but in till that has traditionally been equated with an earlier “Skipsea Till advance”. This is verified by OSL dates of  $23.6 \pm 1.9$  ka (single grain) and  $20.4 \pm 1.6$  ka (single aliquot) from sands and gravels that have been incorporated into the base of the Skipsea Till at Barmston (Fig. 4a; Shfd10215, Table 1; revised from 18.6 ka and 21.5 ka of Bateman *et al.* 2015). These sediments provide a maximum age on the emplacement of the upper till along the Holderness coast and hence are derived from the chronos-

stratigraphically equivalent inter-till sand dates from Dimlington, which clearly predate the Withernsea Till at its type site. Offshore, the thick accretionary till wedges identified by Dove *et al.* (2017) record the dynamic, quasi-stable oscillation of the NSL during the onset of this period (i.e. Limit 4).

Retreat from Limit 4 was marked by the withdrawal of the NSL from the eastern England coast into the central North Sea. At Barmston this is dated at 20.4–18.0 ka based on single aliquot OSL ages from sands and gravels overlying the Skipsea Till (Shfd10214 and Shfd11007, Table 1; revised from 15.0 ka and 16.3 ka of Bateman *et al.* 2015). The deglaciation of the Lincolnshire Marsh is clearly recorded geomorphologically by the superimposition of glacier karst features (eskers and ice-walled lake plains) on overridden moraine ridges, collectively known as the Hogsthorpe–Killingholme Moraine (Evans *et al.* 2019). This phase of downwasting is dated by OSL ages of  $19.3 \pm 1.4$ – $17.4 \pm 1.1$  ka (Shfd15154 and Shfd15155; Table 1) from sands in one of the many ice-walled lake plains at Thoresthorpe (Fig. 4a). At Sewerby, north of Holderness (Fig. 4a), glaci-fluvial outwash gravels and sands overlying the Skipsea Till are OSL-dated to  $18.6 \pm 1.9$  ka (Shfd05250, Table 1; revised from the 17.9 ka of Bateman *et al.* 2015) and record the final phase of terrestrial deglacial sedimentation in the area. Further north, the later stages of Glacial Lake Pickering sedimentation at East Heslerton (Fig. 4a) are dated to 18.4 ka (Shfd13054 and Shfd13055; revised from the 17.6 ka of Evans *et al.* 2017; Table 1). For both lakes Humber and Pickering, the later stages of sedimentation were likely conditioned as much by moraine-damming as by ice-damming. Lake Pickering was impounded by the Filey and Flamborough Head moraine complexes and Lake Humber by the Elloughton/Ferriby/Horkstow moraine complex until its breaching and incision (cf. de Boer *et al.* 1957; Gaunt *et al.* 1971; Gaunt 1974; Bateman *et al.* 2018). Retreat offshore is documented by the sediments of core 137VC (Fig. 4b), within which a radiocarbon age of  $19.8 \pm 0.2$  cal yrs BP (UCIAMS-176372; Roberts *et al.* 2019; Table 1) from deglacial glaci-marine sediments represents a minimum age for deglaciation. The advance and retreat phase boundaries for Limit 4 from the Bayesian model are dated 19.7 and 19.5 ka, respectively (Fig. 7a).

Further north, at Seaham on the Durham coast (Fig. 4a), OSL ages of  $19.9 \pm 2.3$ – $19.1 \pm 1.9$  ka (Shfd14064–Shfd14066; Roberts *et al.* 2019; Table 1) can be used to chronologically constrain both the retreat from Limit 4 and the subsequent advance to Limit 5, because they are derived from glaci-fluvial outwash sands and gravels between two tills (Fig. 4a). In addition to the upper till at Seaham, the sediments of offshore core 132VC also record the advance to Limit 5 and include glaci-marine deposits dated to younger than  $19.6 \pm 0.2$  cal yrs BP (SUERC-68010; Roberts *et al.* 2019; Table 1) overlain by till. This ice-sheet margin is demarcated by a grounding zone wedge (W1 of Roberts *et al.* 2019) offshore of the Durham coast (Fig. 1). The advance and retreat phase boundaries for Limit 5 from the Bayesian model are dated 18.4 and 17.3 ka, respectively (Fig. 7a).

#### Limit 6 – NSL retreat (~19–16.5 ka)

To the south of core 111VC, there is a spectacular series of north–south-aligned and infilled tunnel valleys (Figs 1 and 6). These transition westward into a series of seafloor ridges that have for many years been described as the Wee Bankie Moraine complex (Thomson & Eden 1977; Stoker *et al.* 1985; Gatliff *et al.* 1994; Merritt *et al.* 2003). Six distinctive acoustic facies (Wee Bankie (WB)/AF1–5) can be identified (Fig. 5a). There is a clear lower erosion surface across the base of the

moraine complex. Below this (WB)/AF1 is generally acoustically transparent and massive, but in several places sub-horizontally orientated sediment packages occur below this undulatory erosion surface. These may be pre-MIS 2 sediments (Yarmouth Road Formation, Fisher Formation) but could also be MIS 2 tills. None were cored as part of the BRITICE-CHRONO project, hence further investigation is required. The tunnel valley infill (WB)/AF2 contains several cut and fill sequences composed of grey, laminated clays and silts (see core 125VC; Fig. 5a).

Immediately to the west of core location 125VC, the architecture of a valley infill shows shallow delta foresets in a valley-marginal location, prograding into delta bottomsets (Fig. 5a, WB)/AF2; 127VC–118VC). The upper surface of this delta (if marine in origin) provides a possible control on early sea level (91 m below OD) in the central basin. From this point westwards, the seafloor morphology changes, with a series of drowned ice-contact deltas (WB)/AF3; Fig. 5a) marking ice recession into the Firth of Forth. Between cores 121VC and 124VC, the delta foresets are particularly prevalent in the acoustic stratigraphy and, again, if marine in origin their upper surfaces could provide a control on deglacial sea level (e.g. core site 121VC is at 57 m below OD) (see later discussion). These deltas form the core of the outer Wee Bankie Moraine complex and in places the acoustic architecture also shows feeder tunnels/channels and eskers connecting to the deltas (WB)/AF4; Fig. 5c). However, west of core site 120VC the architecture of the seafloor changes, with large, bedrock and till-cored ridges (WB)/AF1) forming prominent moraines. These are draped by laminated clays and silts containing marine fauna (WB)/AF5) and in cores 118VC–120VC, radiocarbon-dating of mixed foram samples and a mollusc sample of *Nuculana pernula* provided minimum deglacial ages for the inner Wee Bankie Moraine complex of  $17.9 \pm 0.2$ ,  $16.6 \pm 0.2$ ,  $18.0 \pm 0.2$  and  $17.6 \pm 0.2$  cal ka BP, respectively (SUERC-68001 and 68007; Roberts *et al.* 2019 and SUERC-68008 & 68883; Table 1). These ages are supported by onshore dates from the Tay and Forth estuaries, where glaci-marine sediments associated with the Errol Beds Formation show that ice had moved west of the present coastline prior to  $16.9 \pm 0.2$ – $16.0 \pm 0.1$  ka (SRR-391, AA-37787, Beta-111508, CAMS-77912 and OxA-1704, Table 1; see Harkness & Wilson 1979; Hedges *et al.* 1989; Peacock & Browne 1998; Peacock 2002; Hughes *et al.*, 2011, for overview).

In summary, retreat from Limit 5 is recorded by dates from glaci-marine sediments in offshore cores 118VC–120VC. Radiocarbon ages from these deglacial deposits range from 18.0 to 16.6 cal yrs BP (Table 1). They lie beyond the W2 grounding zone wedge situated offshore of Berwick and were used by Roberts *et al.* (2019) to demarcate Limit 6. A minimum OSL date of  $16.2 \pm 0.8$  ka from glaci-fluvial outwash at Maiden Castle in Durham City (Fig. 4a; Tables 1, S1; Shfd14067) records the final stages of sedimentation in the Wear valley. Retreat from Limit 6 is also recorded by ice distal glaci-marine sediments from core 128VC, collected from inside the W2 grounding zone wedge offshore of Berwick. A radiocarbon date of  $17.0 \pm 0.2$  cal yrs BP from these sediments (SUERC-68009; Roberts *et al.* 2019; Table 1) is compatible with those from the early deglacial raised marine Errol Beds Formation of the Tay and Forth estuaries, which indicate ice withdrawal from the Scottish east coast in this area prior to  $17.0$ – $16.0$  cal yrs BP (Gallowflat/Kinneil Kerse/Barry Clay Pit, Fig. 4a; Harkness & Wilson 1979; Hedges *et al.* 1989; Peacock 2002; Table 1). The retreat phase boundary for Limit 6 from the Bayesian model is dated to 15.8 ka (Fig. 7a).

## Northern sector

### Defining and dating pre-LGM ice extent

The glacial history of eastern Scotland is complex and much debated. For many years it was argued that the eastern areas of Buchan remained ice free during MIS 2 (Synge 1956, 1963; Sutherland 1984), but more recently it has been demonstrated that the regions of Buchan and Moray were fully glaciated by ice sourced from the northwest and west and later bounded offshore by large ice streams (Strathmore and Moray Firth ice streams) that flowed into the northern and central North Sea during the later phases of the last glacial cycle. Along the southern edge of the Moray Firth, a number of sites with sandy tills indicate a northwest-to-southeast ice advance across the Moray Firth between ~45.4 and 37.8 ka based on OSL dating of gravel fans (Duller *et al.* 1995). Shelly tills across the lowlands of Buchan and Moray post-date the early sandy tills in this region (Peacock and Merritt, 2000a), and together with erratic trains and striae support southeasterly flow with thick ice over the eastern Grampians and Strathmore. Merritt *et al.* (2017) assign this to 32–24 ka and propose full shelf-edge glaciation of the northern North Sea by this time, with ice over Caithness, Orkney and Shetland coalescent with the FIS. Between 24 and 23 ka, Merritt *et al.* (2017) suggest ice thinning and flow reorganisation over eastern and northeast Scotland. This evidence is linked to flow-set mapping and till superimposition with ice flowing east-northeast/northeast (Merritt & Auton 1993; Fletcher *et al.* 1996; Hall *et al.* 2016a, b). This possibly marks the early onset of the Moray Firth Ice Stream but geochronological control is weak.

The offshore region east of the Firth of Forth is covered in a diverse mosaic of Quaternary sediments (Gatliff *et al.* 1994; Davies *et al.* 2011). The older (>MIS 6) Quaternary sediments infill a complex series of anastomosing tunnel valleys that run north to south (Huuse & Kristensen 2016). Those older sediment sequences include the Yarmouth Road Formation, Fisher Formation and Coal Pit Formation (Davies *et al.* 2011). With respect to constraining ages on LGM onset, there is a single radiocarbon age of  $36.8 \pm 0.7$  ka (SRR-637) from a piece of lignitised wood in cold shallow marine sediments associated with the Aberdeen Ground Beds, 300 km east of the Firth of Forth (Holmes 1977).

In the northern sector of the North Sea, the onset of MIS 2 glaciation is constrained by several radiocarbon ages in the Fladen and Witch Ground areas, which limit ice build-up to post-33 ka. In particular, Graham *et al.* (2010) report reworked forams and shell fragments in overrun glacimarine sediments in core BGS BH 04/01, which range from 35.2 to 32.4 ka. Associated with this, Graham *et al.* (2010) report the production of mega-scale glacial lineations (MSGL) as ice streamed northwest along the suture zone between the FIS and BIIS, though the exact position and longevity of coalescence between the BIIS and FIS remain contentious. Sejrup *et al.* (1994) also report reworked shells in till to the east of the Witch Ground to  $37.0 \pm 0.7$  (Table 1; TUA-274). Hughes *et al.* (2016) reconstruct coalescence between ~27 and 19 ka based on the available chronology. In contrast, Patton *et al.* (2016, 2017) limit coalescence to a brief window ~23–22 ka based on a 3D thermomechanical model validated against geomorphological, geochronological and sea-level datasets. Sejrup *et al.* (2016) suggest a longer coalescence period between 23 ka and 19 ka.

In the central sector of the North Sea (east of the Firth of Forth), glacial sediment sequences and landforms relating to MIS 2 glaciation are very poorly constrained. The Wee Bankie Moraine complex (and associated sediments) is situated ~50 km east of St Andrews, and marks ice retreat

from the central North Sea, but beyond this the ice extent in the central North Sea during MIS 2 remains largely unexplored. Stoker *et al.* (1985) and Cameron *et al.* (1987) report the widespread occurrence of the Forth Formation in this region, which is a deglacial phase glacimarine drape that covers much of the seafloor, but there are few reports of subglacial or ice-marginal sediments that fix BIIS ice extent or provide evidence for coalescence with the FIS.

Between ca. 22 and 19 ka, Merritt *et al.* (2017) suggest Moray Firth ice thickened along the Moray and Buchan coasts, as the Strathmore Ice Stream began to feed ice northwards from the inner Firth of Forth. This is evidenced by the red tills, striae and subglacial bedforms along the eastern margin of the ice stream. It is highly likely that the BIIS and FIS remained coalescent across the central and northern North Sea at this time. Radiocarbon dates from the Witch Ground Basin cores (Sejrup *et al.* 2015) do not necessarily support early marine inundation between 25 and 19 ka and the Wee Bankie Moraine complex relates to a later period of ice-marginal stabilisation (Roberts *et al.* 2019; see *Discussion* below). The latter stages of recession in the region are also marked by ice thinning along the southern Moray and Buchan coasts and the development of ice-marginal lakes (glacial lakes Ugie and Ythan; Merritt *et al.* 2017). The east Grampian sector of the BIIS receded under cold-based conditions at this time, as evidenced by abundant ice-marginal meltwater channels.

### Deglaciation of the central North Sea (18–15.2 ka; retreat through Limits 5 and 6)

The timing and nature of deglaciation in the northern North Sea is complex. Along the western margin of the NCIS between Ling Bank and the Viking Bank/Plateau, grounding zone wedges suggest ice initially deglaciated southward as the NCIS waned (Figs 1 and 5). However, the Tampen Ridge (Fig. 3) indicates re-expansion of the NCIS early during deglaciation. It has recently been hypothesised that the Ling Bank may have acted as a spillway for the decanting of the Dogger Lake (the Dogger Lake Uncoupling Event or DLUE) northwards as the FIS and BIIS uncoupled (Sejrup *et al.* 2016), and a new chronology based on an oxygen isotope anomaly related to the meltwater plume has fixed this event at 18.7 ka (Hjelstuen *et al.* 2018). This would mark the initial uncoupling of the BIIS and FIS at ~19 ka and suggests that the BIIS and FIS uncoupled along a south-to-north trajectory. Cores collected during the BRITICE-CHRONO cruise JC123 in the North Sea confirm that subglacial tills to the north of Ling Bank are draped by glacimarine sediments, but the oldest constraining date on deglaciation was  $14.5 \pm 0.3$  ka (SUERC-67989) from core 097VC from the northern edge of the Ling Bank (Table 1). However, the early onset and timing of marine inundation can be established using several lines of other evidence. Drowned cusped foreland shorelines at 106 m below OD south of the Ling Bank further allude to very early marine inundation of this sector of the North Sea. This is consistent with BRITICE-CHRONO sea-level reconstructions generated using the output of a regional ice-sheet model incorporated into a glacial-isostatic adjustment model (Ely *et al.* 2019), the model being validated using ice margins identified herein for the BIIS and the DATED ice margins for the FIS (Hughes *et al.* 2016) (Fig. 8).

The drowned deltas reported from further west on the seafloor between cores 121VC and 125VC (Figs 5c and 8) also help to constrain the nature and timing of marine inundation during initial deglaciation. As with the cusped foreland, deltas 1 and 2 must represent drowned landscapes as they do not intersect relative sea level (Fig. 8). In order for it to be preserved, the cusped foreland must have been instantaneously drowned

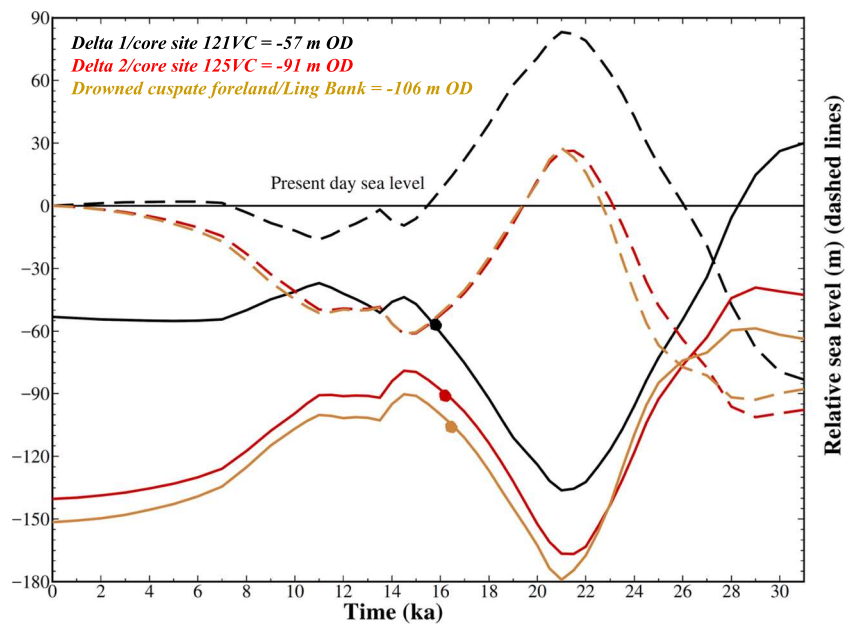


**Figure 8.** Predicted relative sea level (dashed) and water depth (solid) at three sites: core 121VC (black line; 56.42°N, 1.64°W), core 125VC (red line; 56.68°N, 1.3°E) and Ling Bank (brown line; 58.75°N, 3.5°E). Model output is generated from a glacial-isostatic adjustment model updated to include the latest regional ice-sheet reconstruction (BIIS and FIS) from BRITICE-CHRONO. The water depth is calculated by subtracting the predicted relative sea level from present-day bathymetry.

following BIIS/FIS decoupling; in contrast, the deltas are dominated by foreset-type acoustic stratigraphy, inferring ice-contact sedimentation into deep water as the BIIS grounding line retreated to the west. Taking into account our new regional framework for regional deglaciation, the cusplate foreland and deltas can be assigned an age of ~19–17 ka (Figs 5c and 8).

The initial retreat of the BIIS westward through the Fladen and Witch Ground regions is constrained by moraines and glacial debris flows that mark ice margin oscillation. They are dated using two cores (BGS 77/2 and BGS BH 04/01; Graham *et al.* 2010; Sejrup *et al.* 1994, 2015; Fig. 4b) but age reversals hinder a simple interpretation. Throughout both cores both foram and shell ages reverse consistently. This relates either to the reworking of older material, contamination by old carbon or bioturbation. In core BGS BH 04/01, a grounding line efflux unit has two dates  $19.6 \pm 0.4$  and  $16.8 \pm 0.1$  cal ka BP (Ua-32760 and Beta-225422; Table 1). These are very similar to two dates from the lower glacial unit in BGS 77/2, which date to  $19.5 \pm 0.3$  and  $17.7 \pm 0.2$  cal ka BP (TUa-141 and TUa-459). Taken together they bracket the Fladen 1 Moraine (Sejrup *et al.* 2015; Figs 1, 6) and would fit with a DLUE. To the northeast and northwest of the Fladen 1 Moraine, a more prominent moraine (Fladen 2; Fl2 in Figs 1 and 6) is bracketed by three cores in glacial marine sediment (BGS core 58+00/111; Witch Ground Basin 58°34.5'N, 00°24.1'E; Long *et al.*, 1986); GS140-05-14GC and GS140-05-15GC; Sejrup *et al.*, 2015), all of which provide minimum constraints on deglaciation ( $15.9 \pm 0.2$ ,  $16.2 \pm 0.1$  and  $14.6 \pm 0.2$  cal ka BP, respectively) (Table 1). It should be noted that GS140-05-14GC is characterised by age reversals. To the south of GS 140-05-15GC, a glacial debris flow, potentially sourced from the east, has been linked to a "Tampen Readvance" margin by Sejrup *et al.* (2015) but geomorphologically this is difficult to substantiate. To summarise, the key offshore moraine margins that constrain BIIS/FIS uncoupling and grounding line recession under glacial marine conditions are Fladen 1 and 2 which lie in a time window from 19.5 cal ka BP to 16.2 cal ka BP (Sejrup *et al.* 1994, 2015; Graham *et al.* 2010). Here we equate moraine margins Fladen 1 and 2 (Sejrup *et al.* 2015) with Limits 5 and 6 based on their chronological overlap. The advance and retreat phase boundaries for Limit 5 (Fladen 1) are dated to 18.0–17.4 ka

using the Bayesian model, while Limit 6 (Fladen 2) is dated to 16.3–15.2 ka (Fig. 7b).

South of the Witch Ground Basin region, in the central North Sea, a series of cores (JC123: 111VC–117VC) and geophysical data from BRITICE-CHRONO cruise JC123 (Fig. 5b) shed further light on possible ice-marginal positions as the BIIS decoupled from the FIS in the vicinity of the Great Fisher Bank (Fig. 6). No subglacial tills were recovered in these cores but glacial marine and possible glacial lacustrine sediments drape the seafloor. Six acoustic facies (Great Fisher Bank (GFB)/AF 1–6) were mapped in relation to these cores. GFB/AF1 is a clear lower reflector, possibly of Yarmouth Roads Formation or Fisher Formation origin. Overlying this are a series of on-lapping semi-transparent units of variable thickness (GFB/AF2; Figs 5b and 6). They are often incised by infilled channels/valleys and in places form distinctive 'bumps' on the seafloor, with inclined internal reflectors indicative of thrusting and stacking; hence they are interpreted as moraines within which GFB/AF2 is composed of subglacial till (Fig. 5b, 111VC–117VC). Draping these sediments and infilling numerous valleys is GFB/AF3, a stratified lithofacies composed of laminated fines. In cores 112VC–114VC (Figs 5b and 6), toward the eastern end of the area, an olive grey clay with thin sand lenses and occasional soft sediment deformation structures occurs and is devoid of fauna. At the location of cores 112VC–114VC the seafloor is marked by a distinctive scarp/step with a steeply dipping western face and gently dipping eastward slope (Figs 4b and 5b). The geophysical data from this location show this scarp feature to be composed of folded or dissected GFB/AF3, overlain by gently dipping GFB/AF4 and topped by GFB/AF5 (a silty sand). It has the internal architecture and surface profile of a subaqueous ice-contact fan (e.g. Cheel & Rust 1982; Powell 1990; Lønne 1995). The lack of fauna in cores 112VC–114 VC suggests GFB/AF3 may be of glacial lacustrine origin. The Great Fisher Bank, slightly further east (Fig. 1), on the other hand, is not an ice-contact feature but rather a large sand bar, composed exclusively of Holocene sand; many areas of the seabed are truncated by migrating sand bars. A peat sample from a short core (117VC) just below the seafloor returned a radiocarbon date of  $13.4 \pm 0.1$  cal ka BP (SUERC-72877, Table 1),

constraining the timing of marine inundation in this shallow eastern sector of the North Sea Basin.

Further to the west, core 111VC (Figs 4b and 5c) records a strong basal reflector overlain by several acoustic facies. This site is 150 km west of core site 112VC, hence cross correlation of acoustic facies is not feasible. The cores from 111VC heading north to 104VC are given the prefix Bosies Bank (BB)/AF1–6. Above the basal reflector several units are transparent to semi-transparent, massive and structureless (BB/AF2). They are also associated with possible moraines and interpreted as subglacial tills. At core site 111VC, a small valley incision was cored and this recovered 5 m of sediment. At the base of the core was a laminated clay/silt overlain by more massive grey/brown clays with sandy inclusions. This unit is assigned to BB/AF3 but contains marine fauna, indicating that it is glacial marine rather than glacial lacustrine. A shell fragment provided a minimum deglacial age of  $17.6 \pm 0.2$  cal ka BP (core 111VC; SUERC-68000; Table 1), consistent with our earlier interpretation that ice was retreating towards Limit 5 (Fladen 1).

#### Limit 7 (~15 ka)

Additional control on the retreat of ice through the Bosies Bank and into the Moray Firth areas comes from cores 104VC–111VC which span a 180 km transect that displays a series of inset moraines marking grounding line retreat towards Bosies Bank (Figs 1 and 5c). The seafloor in this region is composed of six acoustic facies. BB/AF1 is bedrock/pre-MIS 2. It is overlain by two acoustically transparent units BB/AF2 and BB/AF3 that have the geophysical hallmarks of subglacial till (Fig. 5b). In places these two facies form the cores of moraine complexes. Above this, stratified fines (BB/AF4) drape the underlying topography and on-lap the seafloor moraines. These are glacial marine sediments and contain *in situ* glacial marine fauna. Occasionally they are overlain by an upper diamicton (BB/AF5) that is interpreted as subglacial till relating to ice margin oscillation (see core 104VC). Above BB/AF4 and BB/AF5 the sequence is capped by a thin silty sand with ubiquitous shell fragments, which is a product of Holocene-to-recent seafloor processes (BB/AF6). Three cores provide minimum ages on ice retreat towards the Bosies Bank moraine complex. Cores 104VC–106VC contain four radiocarbon ages on *in situ* forams from glacial marine sediments overlying tills, which cluster at  $\sim 15.0$  cal ka BP (SUERC-67990–67992 and 67997, Table 1). These tie in with ages from the Witch Ground Basin slightly further east where retreat began prior to 16.2 cal ka BP.

Graham *et al.* (2009) suggest ice was flowing east/south-eastwards towards the Witch Ground Basin prior to retreat to the Halibut and Bosies Bank moraine complexes (Fig. 1), although Finlayson *et al.* (2014) also show convincing evidence for MSGL orientated more southwest to northeast. Bosies Bank and Halibut Bank are related to a period of ice margin stability or readvance, or possibly a surge, with Graham *et al.* (2009) reporting evidence for ice-marginal glacial tectonics as well as stagnation under rising sea-level conditions. West of Bosies Bank the seafloor is crosscut by a spectacular set of rock cut subglacial channels trending east to west. Further west, the Elgin Moraine (Peacock, 1968) and De Geer moraines along the coast at Tarbert Ness (Fig. 1) suggest glacial marine conditions along the Moray Firth Ice Stream margin as it retreated landward in a sea level that was at  $\sim 55$  m OD (Finlayson *et al.* 2014). Radiocarbon dates on marine bivalves in glacial marine deposits at St Fergus suggest ice margin oscillation after 17.5 cal ka BP (Beta-101953, Lu-3028; Table 1). Four other radiocarbon ages from a core (Moray Firth/73/75) just north of the Banff coast limit ice retreat through this area to 20.2–17.0 cal ka BP (SRR-322–SRR-325; Table 1). However, the Bayesian analysis suggests that the majority of these are outliers and hence

anomalously old (Fig. 7b). Offshore, core 74/18 in the centre of the Moray Firth also contains glacial marine sediments dated to  $13.9 \pm 0.1$  cal ka BP (Harkness and Wilson, 1979), providing the only viable limiting deglacial age for this area according to the Bayesian model (Figs 6 and 7). The Bayesian model constrains Limit 7 to 15.0 ka with deglaciation of the inner Moray Firth by 13.5 ka.

Deglaciation of the Buchan coast under glacial marine conditions is inferred from glacial marine deposits and nearshore De Geer moraines lying just offshore between St Fergus and Lunan Bay (Bradwell *et al.* 2008), which suggest that the Strathmore Ice Stream began to retreat under marine conditions. Its northward trajectory at this late stage was likely a result of thinning and topographic confinement, or alternatively, it formed the northern sector of a much larger Firth of Forth piedmont lobe (Roberts *et al.* 2019). Previous reconstructions highlight glacial marine clays at Lunan Bay dated to 20.1–20.9 cal ka BP (McCabe *et al.* 2007) as indicative of ice-free conditions on the central Buchan coast, but this would signify a very early collapse of the Strathmore Ice Stream and early marine inundation of the northern and central North Sea Basin (Sejrup *et al.* 2015). This is incompatible with the regional offshore deglacial history presented here and with sea-level reconstructions by Shennan *et al.* (2006, 2018), which indicate that the area only became ice-free after  $\sim 16$ –17 ka.

## Discussion: regional palaeoglaciological reconstruction

Based upon the details outlined above and their reconciliation with wider palaeoglaciological reconstructions pertaining to northern England and eastern Scotland we can now address the key research questions posed in the introduction to this study.

### How far did the BIIS extend?

The southernmost limit of the NSL is recorded offshore by the Bolders Bank Formation south of the Dogger Bank (Limit 1) and onshore by the Garret Hill Moraine in north Norfolk (Limit 3). Limit 1 is dated to 31.4–25.3 ka by OSL dates overlying Bolders Bank Formation till in several cores (138VC–141VC, 178VC and 179VC; Roberts *et al.* 2018). Ice-marginal oscillations between 28 and 22 ka in the Dogger Bank region then produced several additional Bolders Bank Formation tills and it is these that overprint the seafloor down to Limit 3, forming the Hunstanton Till limit and Garret Hill Moraine on the Norfolk coast at 21.5–20.7 ka. Hence Limits 1 and 3 are partially to totally overprinted at the southern extent of the BIIS, as recently demonstrated by Dove *et al.* (2017). This overprinting is likely manifest also in the complex till stratigraphies and inset moraines along the Lincolnshire and East Yorkshire coast (i.e. Skipsea Till, Marsh Tills, Hunstanton Till, Stickney Moraine and Horkstow Moraine) and in the seafloor sedimentary architecture as the ice withdrew northwards towards Limit 4 (Dove *et al.* 2017). The existence of ice-dammed lakes along the east coast while the NSL occupied Limits 1–3 is reinforced by several OSL dates (e.g. 24.1–22.3 ka) limiting the development of Glacial Lake Humber (Bateman *et al.* 2000, 2015; Murton *et al.* 2009). In our model the Vale of York lobe occupied the York/Escrick moraines at ca. 21.5–20.7 ka (Limit 3) but potentially extended further south for a short period prior to this.

In the central North Sea, the extent of the BIIS remains largely unconstrained but has been regarded as coalescent with the FIS over the area of the Great Fisher Bank and along the western edge of the NCIS. Reported ages on this have varied, but include ice-sheet build-up from 35.2 ka to 32.4 ka (Graham *et al.* 2010) and coalescence in the time windows of

30–23 ka (Sejrup *et al.* 2016), ~27–19 ka (Hughes *et al.* 2016), and ~23–22 ka (Patton *et al.* 2016, 2017). Coalescence is supported by the production of MSGL recording the development of a suture zone between the FIS and BIIS with ice flow towards the northwest.

### *How, when and where did the BIIS and FIS uncouple?*

Sejrup *et al.* (2016) proposed regional decoupling of the BIIS and FIS together with rapid flow instability between 19 and 17.5 ka, which they associated with the retreat of the NCIS and the catastrophic northerly drainage of the Dogger Lake complex. This was further constrained by Hjelstuen *et al.* (2018), who identified a distinct freshwater meltwater spike dated to 18.7 ka. However, Roberts *et al.* (2019) have questioned the veracity of these age estimates, as there are several deglacial radiocarbon ages derived from glacial marine sediments from the central North Sea that suggest marine inundation of this region by 19.9–19.5 ka (Table 1). The first evidence of the development of a BIIS ice-marginal feature in relation to decoupling is found at core sites 112VC–114VC, where a drowned ice-contact fan occurs on the seafloor and is associated with a glacial lake lying to the east of the Great Fisher Bank. This feature is not presently dated but is constrained by a minimum peat radiocarbon date of  $13.4 \pm 0.1$  cal ka BP (SUERC-72877; Table 1).

### *Did marine inundation of the northern North Sea destabilise the BIIS and thereby trigger rapid east-to-west retreat?*

The retreating BIIS margin is demonstrably marine tidewater in nature at and after the attainment of Limit 5 (18.4–17.3 ka; Bayesian model). Therefore, this question can be addressed only in relation to the later stages of retreat in both the central and northern North Sea. It should be noted that prior to this, the BIIS margin in the North Sea was exclusively terrestrially based and/or in contact with glacial lakes. The trigger for inundation may have been the combined effects of the NCIS retreating eastwards and the opening of the Dogger Lake spillway in the time window of 19.9–17.5 (see above; cf. Sejrup *et al.* 2016; Roberts *et al.* 2019).

In the southern sector of the North Sea, as the ice retreated north of the Yorkshire coast and Dogger Bank, there is the first clear evidence for glacial marine sediment draping tills as well as morainal banks and grounding zone wedges. These all clearly relate to the transition from terrestrial glaciation to fully marine ice margins at which the construction of grounding zone wedges in particular indicates re-equilibration in deepening marine water. The earliest dates on these landform-sediment assemblages come from cores 132VC and 137VC (19.8–19.6 ka). Further dating constraint is provided by the OSL ages of 19.9–19.1 ka from glacial fluvial sediments between tills at Seaham. Recession of this ice margin continued into the Firth of Forth from Limits 5 to 6, also characterised by the continued deposition of glacial marine sediments over a mixed-bed subglacial imprint (Roberts *et al.* 2019). More importantly, only one further grounding zone wedge is reported off the coast of Berwick and with a deglacial date of  $17.0 \pm 0.2$  cal ka BP (core 128VC), inferring rapid retreat in contact with marine water. Final deglaciation of the inner Firth of Forth under glacial marine conditions is recorded by the Errol Beds of the Tay and Forth estuaries, which indicate ice withdrawal in this area by 16.9–16.0 ka.

Further evidence of rapid recession in contact with marine conditions occurs in the Fladen and Witch Ground basins. For

example, in cores BGS BH 04/01 and BGS 77/2, proximal glacial marine sediments are dated to 19.5–16.8 ka. These dates bracket the Fladen 1 Moraine, demonstrating uncoupling from the FIS, clear ice margin recession of the BIIS, and marine inundation. These ages overlap with the age of the DLUE at 18.7 ka. Further ice recession between Limits 5 and 6 is marked by the Fladen 2 Moraine, which is dated at approximately 16.2 ka. Ice retreat under marine conditions is further reinforced by evidence of ice-marginal recession through the Wee Bankie Moraine complex and into the Firth of Forth, with the ice-contact deltas on the seafloor marking ice retreat through deep water between 19 and 17 ka (Fig. 8). Continued recession from Fladen 2 to the Bosies Bank/Halibut Bank moraines is constrained by a cluster of dates around ~15 ka. These dates suggest that the Moray Firth Ice Stream may have occupied the inner continental shelf for slightly longer than ice in the Firth of Forth. Further west, as the Moray ice moved onshore, glacial marine sediments and De Geer moraines indicate the continued instability of the ice margin under tidewater conditions, although the timing of this is not well constrained (15–13 ka; see details above).

### *What are the major BIIS controls on North Sea ice flow dynamics and deglaciation patterns?*

Firth of Forth ice was the dominant source for the NSL even during deglaciation. Smaller ice streams such as the Stainmore, Tyne Gap and Tweed have no significant imprint offshore in the North Sea and had uncoupled from the NSL by ~18 ka (Livingstone *et al.* 2015; Davies *et al.* 2019). Ice-marginal landforms running sub-parallel and inboard of the Northumberland coast demonstrate uncoupling of the western flank/suture zone of the NSL from inland ice streams (Teasdale, 2013), while the NSL retreated northward offshore and back into the Firth of Forth (Roberts *et al.* 2019). The deglaciation of the NSL was heavily influenced by the transition from terrestrial to marine conditions with a dynamic, quasi-unstable terrestrial margin, initially producing overprinted till sheets (Dove *et al.* 2017), before grounding zone wedges developed in response to further instability driven by marine inundation (Roberts *et al.* 2019). The possible 'surge-like' imprint of the NSL has been noted by many authors and this may be related to marginal instability. It is also possible that changes in the topographic configuration of the southern North Sea Basin in relation to the glacitectonism of the Dogger Bank, accentuated the dynamic behaviour of the NSL after ~23 ka (Roberts *et al.* 2018).

In the northern North Sea Basin, the Moray Firth drainage basin was extremely influential in determining ice retreat from the Fladen/Witch Ground areas westwards through the Bosies and Halibut Bank regions from 18 to 15 ka. However, the influence of ice sourced from the Orkneys and Shetland during early deglaciation of the northern North Sea requires further investigation. Bradwell *et al.* (2019) have dated initial retreat north of the Fladen/Witch Ground areas to ~20–21 ka. This is problematic if the DLUE occurred at ~19 ka and is earlier than the deglacial dates discussed here for the Fladen 1 and 2 moraines (Limits 5 and 6). However, mapped ice margin configurations clearly show the influence of independent ice caps over Orkney and Shetland during the latter stages of the downwasting of the BIIS. Hence, the ice-sheet history of the central and southern North Sea was strongly dominated by the Firth of the Forth and evolution of the NSL from 31 to 21 ka. Between 21 and 15 ka the southern and central North Sea deglaciated, first under terrestrial conditions but the basin transitioned to marine conditions at ~19 ka. This triggered late stage instability and dynamic flow reorganisation, with Firth of

Forth ice dominating the central North Sea while Moray ice evacuated the Fladen/Witch Ground areas and retreated west; Shetland/Orkney ice deglaciated northward back to local ice centres fringing the northern North Sea.

## Conclusions

The outcomes of the BRITICE-CHRONO Transect 2 through the North Sea Basin and onto the onshore areas of eastern England have facilitated a significantly refined palaeoglaciological reconstruction of the eastern sector of the BIIS and its relationship with the FIS during MIS 2, in a region where ice dynamics were strongly influenced by the transition from terrestrial to marine conditions (Fig. 6). The glacial landsystem imprints of this region comprise substantial arcuate moraine sequences and associated glacial lake plains representative of the interaction and onshore flow of lobate ice streams, the most significant being the NSL, which flowed some 400 km from southern Scotland down the eastern margin of the North Sea Basin to north Norfolk. The interdigitation of glacial till and morainic deposits and stratified sediments, in both onshore stratigraphic outcrops and offshore cores, provided numerous suitable targets for OSL and radiocarbon dating from which a chronology of ice-marginal recession and oscillation has been constructed. This glacial land-systems record and its geochronological control have constrained ice-sheet fluctuation in the time window ~31–16 ka and identified seven distinctive former ice-sheet limits (L1–L7), the latter defined by Bayesian statistical analysis which verified the use or exclusion of some dates where they represented obvious outliers (Fig. 7).

Limit 1 is the most extensive MIS 2 margin and is demarcated offshore by the Bolders Bank Formation south of the Dogger Bank. It relates to the advance of the NSL and dates to some time prior to 31–25 ka. Retreat from Limit 1 is dated at 26–29 ka. The advance and retreat phase boundaries for Limit 1 from the Bayesian model are dated to 25.8 ka and 24.6 ka, respectively. Limit 2 represents NSL oscillation at ~26–24 ka and retreat at ~22 ka. The advance and retreat phase boundaries for Limit 2 from the Bayesian model are dated 23.5 ka and 22.2 ka, respectively. Limit 3 records NSL advance dated to ~21.5 ka, including the construction of the Garrett Hill Moraine in north Norfolk, and initial retreat, with the advance and retreat phase boundaries from the Bayesian model being calculated at 21.5 ka and 20.8 ka, respectively. Limits 4 to 5 relate to NSL oscillation and retreat, incorporating the long-established Withernsea Till emplacement event, and date to ~20–17.2 ka. The advance and retreat phase boundaries for Limit 4 from the Bayesian model are dated to 19.7 ka and 19.5 ka, respectively, and for Limit 5 are dated to 18.4 ka and 17.3 ka, respectively. Limit 6 relates to NSL retreat dating to ~19–16.5 ka and includes the construction of the W2 grounding zone wedge offshore of Berwick. The retreat phase boundary for Limit 6 from the Bayesian model is dated to 15.8 ka. Also related to Limits 5 and 6 is the deglaciation of the central North Sea which dates to 18–15.2 ka. This includes the uncoupling of the BIIS and FIS and grounding line recession under glacial marine conditions, as represented by moraines Fladen 1 and 2 (Limits 5 and 6, respectively). The advance and retreat phase boundaries for Limit 5 (Fladen 1) are dated to 18.0–17.4 ka, using the Bayesian model, while Limit 6 (Fladen 2) is dated to 16.3–15.2 ka. Finally, Limit 7 (~15.0 ka) represents ice retreat from Bosies Bank into the Moray Firth from the central North Sea. Radiocarbon ages from deglacial glacial marine deposits range from 19.6 to 16.4 ka but the majority of these are outliers. Final ice retreat into the Moray Firth is constrained by the Bayesian model to 15.0–13.5 ka.

The deglaciation of the North Sea region was heavily influenced by the transition from terrestrial to marine conditions with a dynamic, quasi-unstable terrestrial margin, initially producing overprinted till sheets, before grounding zone wedges developed in response to further instability driven by the later marine inundation. Previous proposals that the NSL was characterised by repeat surging behaviour is compatible with the marginal instability highlighted by the palaeoglaciological reconstructions presented in this study, but changes in the topographic configuration of the southern North Sea Basin in relation to the glacetectonism of the Dogger Bank may also have accentuated the dynamic behaviour of the NSL after ~23 ka.

## Supporting information

Additional supporting information may be found in the online version of this article at the publisher's web-site.

*Acknowledgements.* This work was supported by the Natural Environment Research Council consortium grant BRITICE-CHRONO NE/J009768/1. Thanks are due to the technical support staff at Sheffield Luminescence Laboratory. Thanks to Sally Morgan and Elke Hanenkamp (University of Leicester) for acquisition and processing of the multi-sensor core-logger data. We acknowledge the crew of the RRS James Cook for technical support during cruise JC123. We thank the many landowners for access to sites along the east coast of Britain. Thanks to Chris Orton and Caroline Roberts (Durham University) for help with figures. Comments provided by Alistair Graham and Arjen Stroeven are greatly appreciated.

## Data availability statement

All relevant data will be made available in the forthcoming BRITICE-CHRONO online data repository, or upon reasonable request from the lead author.

## References

- Agar R. 1954. Glacial and post-glacial geology of Middlesborough and the Tees estuary. *Proceedings of the Yorkshire Geological Society* **29**: 237–253.
- Allen JD. 1980. Aspects of late-glacial environments in Northern England. (Unpublished B.Ed. dissertation) University of Hull.
- Armstrong M, Paterson IB, Browne MAE 1985. Geology of the Perth and Dundee District. 1:50,000 geological sheets 48W, 48E, 49. Memoirs of the British Geological Survey (Scotland), HMSO, London.
- Beckett SA. 1981. Pollen diagram from Holderness, North Humberside. *Journal of Biogeography* **8**: 177–198.
- Balson PS, Jeffrey DH. 1991. The glacial sequence of the southern North Sea. In *Glacial deposits in Great Britain and Ireland*, Ehlers J, Gibbard PL, Rose J (eds). Balkema: Rotterdam; 245–253.
- Bateman MD, Buckland PC, Carpenter R, Davies S, Frederick CD, Gearey BR, Whitehouse NJ. 2001. Cove farm quarry. In *The Quaternary of East Yorkshire and North Lincolnshire*, Bateman MD, Buckland PC, Frederick CD, Whitehouse NJ (eds). QRA: London; 141–160.
- Bateman MD, Catt JA. 1996. An absolute chronology for the raised beach deposits at Sewerby, E. Yorkshire, UK. *Journal of Quaternary Science* **11**: 389–395.
- Bateman MD, Murton JB, Crowe W. 2000. Reconstruction of the depositional environments associated with the Late Devensian and Holocene coversand around Caistor, N. Lincolnshire, UK. *Boreas* **16**: 1–16.
- Bateman MD, Buckland PC, Chase B *et al.* 2008. The Late-Devensian proglacial Lake Humber: New evidence from littoral deposits at Ferrybridge, Yorkshire, England. *Boreas* **37**: 195–210.
- Bateman MD, Evans DJA, Buckland PC *et al.* 2015. Last Glacial dynamics of the Vale of York and North Sea Lobes of the British and

- Irish Ice Sheet. *Proceedings of the Geologists' Association* **126**: 712–730.
- Bateman MD, Evans DJA, Roberts DH *et al.* 2018. The timing and consequences of the blockage of the Humber Gap by the last British–Irish Ice Sheet. *Boreas* **47**: 41–61.
- Boston CM, Evans DJA, Cofaigh C. Ó. 2010. Styles of till deposition at the margin of the last glacial maximum North Sea lobe of the British–Irish ice sheet: an assessment based on geochemical properties of glacial deposits in Eastern England. *Quaternary Science Reviews* **29**: 3184–3211.
- Boulton GS. 1996a. The origin of till sequences by subglacial sediment deformation beneath mid-latitude ice sheets. *Annals of Glaciology* **22**: 75–84.
- Boulton GS. 1996b. Theory of glacial erosion, transport and deposition as a consequence of subglacial sediment deformation. *Journal of Glaciology* **42**: 43–62.
- Boulton GS, Smith GD, Jones AS *et al.* 1985. Glacial geology and glaciology of the last mid-latitude ice sheets. *Journal of the Geological Society of London* **142**: 447–474.
- Boylan PJ. 1967. The Pleistocene Mammalia of the Sewerby–Hessle buried cliff. *Proceedings of the Yorkshire Geological Society* **36**: 115–125.
- Bradwell T, Stoker MS, Golledge NR *et al.* 2008. The northern sector of the last British Ice Sheet: Maximum extent and demise. *Earth-Science Reviews* **88**: 207–226.
- Bradwell T, Small D, Fabel D *et al.* 2019. Pattern, style and timing of British–Irish Ice Sheet retreat: Shetland and northern North Sea sector. *Journal of Quaternary Science*. <https://doi.org/10.1002/jqs.3163>
- Bremner A. 1943. The glacial epoch in the north-east. In *The Book of Buchan*, Tocher JF (ed). Aberdeen University Press: Aberdeen; 10–30.
- Bronk Ramsey C. 2008. Deposition models for chronological records. *Quaternary Science Reviews* **27**: 42–60.
- Bronk Ramsey C. 2009a. Bayesian analysis of radiocarbon dates. *Radiocarbon* **51**: 337–360.
- Bronk Ramsey C. 2009b. Dealing with outliers and offsets in radiocarbon dating. *Radiocarbon* **51**: 1023–1045.
- Bronk Ramsey C, Lee S. 2013. Recent and planned developments of the program OxCal. *Radiocarbon* **55**: 720–730.
- Busfield ME, Lee JR, Riding JB *et al.* 2015. Pleistocene till provenance in East Yorkshire: reconstructing ice flow of the British North Sea lobe. *Proceedings of the Geologists' Association* **126**: 86–99.
- Cameron T, Stoker M, Long D. 1987. The history of Quaternary sedimentation in the UK sector of the North Sea Basin. *Journal of the Geological Society of London* **144**: 43–58.
- Cameron T, Crosby A, Balson PS *et al.* 1992. United Kingdom offshore regional report: the geology of the southern North Sea. British Geological Survey, 149 pp.
- Carr SJ, Holmes R, van der Meer JJM *et al.* 2006. The last glacial maximum in the North Sea basin: micromorphological evidence of extensive glaciation. *Journal of Quaternary Science* **21**: 131–153.
- Catt JA. 2007. The Pleistocene glaciations of eastern Yorkshire: a review. *Proceedings of the Yorkshire Geological Society* **56**: 177–207.
- Catt JA, Penny LF. 1966. The Pleistocene deposits of Holderness, east Yorkshire. *Proceedings of the Yorkshire Geological Society* **35**: 375–420.
- Charlesworth JK. 1956. The late-glacial history of the highlands and the islands of Scotland. *Transactions of the Royal Society of Edinburgh* **62**: 769–928.
- Cheel RJ, Rust BR. 1982. Coarse grained facies of glacio-marine deposits near Ottawa, Canada. In *Research in Glaciolacustrine Systems*, Davidson-Arnott R, Nickling W, Fahey BD (eds). Geobooks: Norwich, UK; 279–295.
- Chiverrell RC, Thrasher IM, Thomas GSP *et al.* 2013. Bayesian modelling the retreat of the Irish Sea Ice Stream. *Journal of Quaternary Science* **28**: 200–209.
- Clark CD, Evans DJA, Khatwa A *et al.* 2004. Map and GIS database of glacial landforms and features related to the last British Ice Sheet. *Boreas* **33**: 359–375.
- Clark CD, Hughes ALC, Greenwood SL *et al.* 2012. Pattern and timing of retreat of the last British–Irish Ice Sheet. *Quaternary Science Reviews* **44**: 112–146.
- Clark CD, Ely JC, Greenwood SL *et al.* 2018. BRITICE glacial Map, version 2: a map and GIS database of glacial landforms of the last British–Irish ice sheet. *Boreas* **47**: 11–27.
- Clayton KM. 1957. The differentiation of glacial drifts in the Midlands. *East Midland Geographer* **1**: 31–40.
- Davies BJ, Roberts DH, Ó Cofaigh C *et al.* 2009. Interlobate ice-sheet dynamics during the last glacial maximum at Whitburn Bay, County Durham, England. *Boreas* **38**: 555–578.
- Davies BJ, Roberts DH, Bridgland DR *et al.* 2011. Provenance and depositional environments of Quaternary sediments from the western North Sea basin. *Journal of Quaternary Science* **26**: 59–75.
- Davies BJ, Roberts DH, Bridgland DR *et al.* 2012. Dynamic Devensian ice flow in NE England: a sedimentological reconstruction. *Boreas* **41**: 337–336.
- Davies BJ, Livingstone SJ, Roberts DH *et al.* 2019. Dynamic ice stream retreat in the central sector of the last British–Irish Ice Sheet. *Quaternary Science Reviews* **225**: 105989.
- de Boer G, Neale JW, Penny LF. 1957. A guide to the geology of the area between Market Weighton and the Humber. *Proceedings of the Yorkshire Geological Society* **31**: 157–209.
- Dove D, Evans DJA, Lee JR *et al.* 2017. Phased occupation and retreat of the last British–Irish Ice Sheet in the southern North Sea: geomorphic and seismostratigraphic evidence of a dynamic ice lobe. *Quaternary Science Reviews* **163**: 114–134.
- Duller GAT, Wintle AG, Hall AM. 1995. Luminescence dating and its application to key pre-Late Devensian sites in Scotland. *Quaternary Science Reviews* **14**: 495–519.
- Ely JC, Clark CD, Hindmarsh RCA *et al.* 2019. Recent progress on combining geomorphological and geochronological data with ice sheet modelling, demonstrated using the last British–Irish Ice Sheet. *Journal of Quaternary Science*. <https://doi.org/10.1002/jqs.3098>
- Emery AR, Hodgson DM, Barlow NLM *et al.* 2019. Left High and Dry: Deglaciation of Dogger Bank, North Sea, Recorded in Proglacial Lake Evolution. *Frontiers in Earth Science*. <https://doi.org/10.3389/feart.2019.00234>
- Evans DJA, Benn D. 2004. *A Practical Guide to the Study of Glacial Sediments*. Arnold: London.
- Evans DJA, Hansom JD. 1996. Scottish Landform Examples - 15: The Edinburgh Castle crag and tail. *Scottish Geographical Magazine* **112**: 129–131.
- Evans DJA, Rea BR. 1999. Geomorphology and sedimentology of surging glaciers: a land-systems approach. *Annals of Glaciology* **28**: 75–82.
- Evans DJA, Rea BR. 2003. Surging glacier landsystem. In *Glacial landsystems*, Evans DJA (ed). Arnold: London; 259–288.
- Evans DJA, Thomson SA. 2010. Glacial sediments and landforms of Holderness, eastern England: a glacial depositional model for the North Sea Lobe of the British–Irish Ice Sheet. *Earth Science Reviews* **101**: 147–189.
- Evans DJA, Owen LA, Roberts DH. 1995. Stratigraphy and sedimentology of Devensian (Dimlington–Stadial) glacial deposits, East Yorkshire, England. *Journal of Quaternary Science* **10**: 241–265.
- Evans DJA, Clark CD, Mitchell WA. 2005. The last British Ice Sheet: a review of the evidence utilised in the compilation of the Glacial Map of Britain. *Earth Science Reviews* **70**: 253–312.
- Evans DJA, Livingstone SJ, Vieli A *et al.* 2009. The palaeoglaciology of the central sector of the British and Irish Ice Sheet: reconciling glacial geomorphology and preliminary ice sheet modelling. *Quaternary Science Reviews* **28**: 740–758.
- Evans DJA, Bateman MD, Roberts DH *et al.* 2017. Glacial Lake Pickering: stratigraphy and chronology of a proglacial lake dammed by the North Sea Lobe of the British–Irish Ice Sheet. *Journal of Quaternary Science* **32**: 295–310.
- Evans DJA, Roberts DH, Bateman MD *et al.* 2018. Sedimentation during MIS 3 at the eastern margins of the Glacial Lake Humber basin, England. *Journal of Quaternary Science* **33**: 871–891.
- Evans DJA, Roberts DH, Bateman MD *et al.* 2019. A chronology for North Sea Lobe advance and recession on the Lincolnshire and Norfolk coasts during MIS 2 and 6. *Proceedings of the Geologists' Association* **130**: 523–540.
- Everest J, Bradwell T, Golledge N. 2005. Subglacial landforms of the Tweed Palaeo-Ice stream. *Scottish Geographical Journal* **121**: 163–173.

- Eyles N, Sladen JA, Gilroy S. 1982. A depositional model for stratigraphic complexes and facies superimposition in lodgement tills. *Boreas* **11**: 317–333.
- Eyles N, McCabe AM, Bowen DQ. 1994. The stratigraphic and sedimentological significance of Late Devensian ice sheet surging in Holderness, Yorkshire, UK. *Quaternary Science Reviews* **13**: 727–759.
- Fairburn WA, Bateman MD. 2016. A new multi-stage recession model for Proglacial Lake Humber during the retreat of the Last British and Irish Ice sheet. *Boreas* **45**: 133–151.
- Farrington A, Mitchell GF. 1951. The end moraine north of Flamborough Head. *Proceedings of the Geologists' Association* **62**: 100–106.
- Finlayson A, Fabel D, Bradwell T *et al.* 2014. Growth and decay of a marine terminating sector of the last British Irish Ice Sheet. *Quaternary Science Reviews* **83**: 28–45.
- Fletcher TP, Auton CA, Highton AJ *et al.* 1996. Geology of the Fortrose and eastern Inverness district. British Geological Survey Memoir for Sheet 84, WHMSO, London.
- Ford JA, Cooper AH, Price SJ *et al.* 2008. Geology of the Selby district – a brief explanation of the geological map. Sheet Explanation of the British Geological Survey, 1: 50,000 Sheet 71 Selby (England and Wales).
- Friend R, Buckland PC, Bateman MD *et al.* 2016. The 'Lindholme Advance' and the extent of the Last Glacial Maximum in the Vale of York. *Mercian Geologist* **19**: 18–25.
- Galbraith RF, Roberts RG, Laslett GM *et al.* 1999. Optical dating of single and multiple grains of quartz from Jinnium rock shelter, northern Australia: Part I, experimental design and statistical models. *Archaeometry* **41**: 339–364.
- Gatliff R, Richards P, Smith K *et al.* 1994. United Kingdom offshore regional report: the geology of the central North Sea. HMSO for the British Geological Survey: London.
- Gaunt GD. 1974. A radiocarbon date relating to Lake Humber. *Proceedings of the Yorkshire Geological Society* **40**: 195–197.
- Gaunt GD. 1981. Quaternary history of the southern part of the Vale of York. In *The Quaternary in Britain*, Neale J, Flenley J (eds). Pergamon: Oxford; 82–97.
- Gaunt GD, Jarvis RA, Matthews B. 1971. The late Weichselian sequence in the Vale of York. *Proceedings of the Yorkshire Geological Society* **38**: 281–284.
- Gaunt GD, Fletcher TP, Wood CJ. 1992. *Geology of the country around Kingston upon Hull and Brigg*. HMSO: London.
- Golledge NR, Stoker MS. 2006. A palaeo-ice stream of the British ice sheet in eastern Scotland. *Boreas* **35**: 231–243.
- Graham AGC, Lonergan L, Stoker MS. 2007. Evidence for Late Pleistocene ice stream activity in the Witch Ground Basin, central North Sea, from 3D seismic reflection data. *Quaternary Science Reviews* **26**: 627–643.
- Graham AGC, Lonergan L, Stoker MS. 2009. Seafloor glacial features reveal the extent and decay of the last British Ice Sheet, east of Scotland. *Journal of Quaternary Science* **24**: 117–138.
- Graham AGC, Lonergan L, Stoker MS. 2010. Depositional environments and chronology of Late Weichselian glaciation and deglaciation in the central North Sea. *Boreas* **39**: 471–491.
- Graham AGC, Stoker MS, Lonergan L *et al.* 2011. The Pleistocene glaciations of the North Sea basin. In *Developments in Quaternary Science: Quaternary Glaciations – Extent and Chronology: a Closer Look*, Ehlers J, Gibbard PL, Hughes PD (eds). Elsevier: Amsterdam; 261–268.
- Guérin G, Mercier N, Adamiec G. 2011. Dose-rate conversion factors: update. *Ancient TL* **29**: 5–8.
- Hall AM, Jarvis J. 1989. A preliminary report on the Late Devensian glacial marine deposits around St. Fergus, Grampian Region. *Quaternary Newsletter* **59**: 5–7.
- Hall AM, Riding JB, Brown JF. 2016a. The last glaciation of Caithness, Scotland: revised till stratigraphy and ice flow paths indicate multiple ice flow phases. *Scottish Journal of Geology* **52**: 77–89.
- Hall AM, Riding JB, Brown JF. 2016b. The last glaciation of Orkney, Scotland: glacial stratigraphy, event sequence and ice flow paths. *Scottish Journal of Geology* **52**: 90–101.
- Harkness DD, Wilson HW. 1979. Scottish universities research and reactor centre radiocarbon measurements III. *Radiocarbon* **21**: 203–256.
- Hedges REM, Housle RA, Law IA *et al.* 1988. Radiocarbon dates from the Oxford AMS system: archaeometry datelist 8. *Archaeometry* **30**: 291–305.
- Hedges REM, Housle RA, Law IA *et al.* 1989. Radiocarbon dates from the Oxford AMS system: archaeometry datelist 9. *Archaeometry* **31**: 207–234.
- Hjelstuen BO, Sejrup HP, Valvik E *et al.* 2018. Evidence of an ice dammed lake outburst in the North Sea during the last deglaciation. *Marine Geology* **402**: 118–130.
- Holmes R. 1977. Quaternary deposits of the central North Sea, 5. The Quaternary geology of the UK sector of the North Sea between 56° and 58°N. Institute of Geological Sciences.
- Hubbard A, Bradwell T, Golledge N *et al.* 2009. Dynamic cycles, ice streams and their impact on the extent, chronology and deglaciation of the British-Irish Ice Sheet. *Quaternary Science Reviews* **28**: 758–776.
- Hughes ALC, Clark CD, Jordan CJ. 2010. Subglacial bedforms of the last British ice sheet. *Journal of Maps* **6**: 543–63.
- Hughes ALC, Clark CD, Jordan CJ. 2014. Flow-pattern evolution of the last British Ice Sheet. *Quaternary Science Reviews* **89**: 148–168.
- Hughes ALC, Greenwood SL, Clark CD. 2011. Dating constraints on the last British-Irish Ice Sheet: a map and database. *Journal of Maps* **7**: 156–184.
- Hughes ALC, Gyllencreutz R, Lohne OS *et al.* 2016. The last Eurasian ice sheets – a chronological database and time-slice reconstruction, DATED-1. *Boreas* **45**: 1–45.
- Huuse M, Kristensen TB. 2016. Pleistocene tunnel valleys in the North Sea Basin. In *Atlas of Submarine Glacial Landforms: Modern, Quaternary and Ancient*, Dowdeswell JA, Canals M, Jakobsson M *et al.* (eds). Geological Society: London, Memoir; 207–208.
- Jamieson TF. 1906. The glacial period between Aberdeenshire and the southern border of the Moray Firth. *Quarterly Journal of the Geological Society* **62**: 13–39.
- Jansen JHF, van Weering TCE, Eisma D. 1979. Late Quaternary sedimentation in the North Sea. In *The Quaternary History of the North Sea*, Oele E, Schuttenhelm RTE, Wiggers AJ (eds). Acta Universitatis, Symposium Universitatis Usaliensis Annum Quingentesimum Celebrantis: 175–187.
- Kendall PF. 1902. A system of glacier-lakes in the Cleveland Hills. *Quarterly Journal of the Geological Society* **58**: 471–571.
- King CAM. 1965. *British Landscapes Through Maps: the Scarborough District*. Geographical Association: Sheffield.
- Lamplugh GW. 1888. Report on the buried cliff at Sewerby. *Proceedings of the Yorkshire Geological and Polytechnic Society* **9**: 381–392.
- Lamplugh GW. 1911. On the shelly moraine of the Sefstrom glacier and other Spitsbergen phenomena illustrative of the British glacial conditions. *Proceedings of the Yorkshire Geological Society* **17**: 216–241.
- Lewis SG. 1999. Eastern England. In *A revised correlation of Quaternary deposits in the British Isles*, Bowen DQ (ed). Geological Society Special Report 23: 10–27.
- Lincoln P, Eddy L, Matthews I *et al.* 2017. The Quaternary of the Vale of Pickering QRA Field Guide. *Quaternary Research Association: London* 190.
- Linton DL. 1959. Morphological contrasts between eastern and western Scotland. In *Geographical Essays in Memory of Alan G. Ogilvie*, Miller R, Watson JW (eds). Edinburgh: Nelson; 16–45.
- Linton DL. 1962. Glacial erosion on soft rock outcrops in central Scotland. *Biuletyn Peryglacjalny* **11**: 247–257.
- Livingstone SJ, Ó Cofaigh C, Evans DJA. 2008. Glacial geomorphology of the central sector of the last British-Irish Ice sheet. *Journal of Maps* **4**: 358–377.
- Livingstone SJ, Ó Cofaigh C, Evans DJA. 2010a. A major ice drainage pathway of the last British-Irish ice sheet: the Tyne Gap, Northern England. *Journal of Quaternary Science* **25**: 354–370.
- Livingstone SJ, Ó Cofaigh C, Evans DJA. 2010b. Sedimentary evidence for a major glacial oscillation and proglacial lake formation in the Solway Lowlands (Cumbria, UK) during Late Devensian deglaciation. *Boreas* **39**: 505–527.
- Livingstone SJ, Evans DJA, Ó Cofaigh C *et al.* 2012. Glaciodynamics of the central sector of the last British-Irish Ice Sheet in Northern England. *Earth Science Reviews* **111**: 25–55.

- Livingstone SJ, Roberts DH, Davies BJ *et al.* 2015. Late Devensian deglaciation of the Tyne Gap Palaeo-Ice stream, northern England. *Journal of Quaternary Science* **30**: 790–804.
- Long D, Bent A, Harland R, Gregory DM, Graham DK, Morton AC. 1986. Late Quaternary palaeontology, sedimentology and geochemistry of a vibrocore from the Witch Ground Basin, central North Sea. *Marine Geology* **73**: 109–123.
- Lønne I. 1995. Sedimentary facies and depositional architecture of ice-contact glacimarine systems. *Sedimentary Geology* **98**: 13–43.
- McCabe AM, Clark PU, Clark J. 2007. Radiocarbon constraints on readvances of the British–Irish Ice Sheet in the northern Irish Sea Basin during the last deglaciation. *Quaternary Science Reviews* **26**: 1204–1211.
- Merritt JW, Auton CA 1993. Notes on exposures and natural sections in drift deposits occurring on Geological Sheet 84W (Fortrose), SE of Inverness, Scotland. British Geological Survey Technical Report WA/93/28R.
- Merritt JW, Auton CA, Connell ER *et al.* 2003. *Cainozoic geology and landscape evolution of north-east Scotland*. Memoir of the British Geological Survey, sheets 66E, 67, 76E, 77, 86E, 87W, 87E, 95, 96W, 96E and 97 (Scotland).
- Merritt JW, Connell RE, Hall AM. 2017. Middle to Late Devensian glaciation of north-east Scotland: implications for the north-eastern quadrant of the last British–Irish ice sheet. *Journal of Quaternary Science* **32**: 276–294.
- Matthews B. 1970. Age and origin of Aeolian sand in the Vale of York. *Nature* **227**: 1234–1236.
- Moorlock BSP, Booth SJ, Hamblin RJO *et al.* 2008. Geology of the Wells-next-the-Sea district – a brief explanation of the geological map, Sheet Explanation of the British Geological Survey. 1:50,000 Sheet 130 (England and Wales).
- Murray AS, Wintle AG. 2000. Luminescence dating of quartz using an improved single-aliquot regenerative-dose protocol. *Radiation Measurements* **32**: 57–73.
- Murray AS, Wintle AG. 2003. The single aliquot regenerative dose protocol: potential for improvements in reliability. *Radiation Measurements* **37**: 377–381.
- Murton DK, Pawley SM, Murton JB. 2009. Sedimentology and luminescence ages of Glacial Lake Humber deposits in the central Vale of York. *Proceedings of the Geologists' Association* **120**: 209–222.
- Nygård A, Sejrup HP, Hafliðason H *et al.* 2005. The glacial North Sea Fan, southern Norwegian Margin: Architecture and evolution from the upper continental slope to the deep-sea basin. *Marine and Petroleum Geology* **22**: 71–84.
- Palmer AP, Matthews IP, Candy *et al.* 2015. The evolution of Palaeolake Flixton and the environmental context of Star Carr, NE. Yorkshire: Stratigraphy and sedimentology of the Last Glacial–Interglacial Transition (LGIT) lacustrine sequences, *Proceedings of the Geologists' Association* **126**: 50–59.
- Patton H, Hubbard AL, Andreassen K *et al.* 2016. The build-up, configuration, and dynamical sensitivity of the Eurasian ice-sheet complex to Late Weichselian climatic and oceanic forcing. *Quaternary Science Reviews* **153**: 97–121.
- Patton H, Hubbard AL, Andreassen K *et al.* 2017. Deglaciation of the Eurasian ice sheet complex. *Quaternary Science Reviews* **169**: 148–172.
- Pawley SM, Candy I, Booth SJ. 2006. The Late Devensian terminal moraine ridge at Garret Hill, Stiffkey valley, north Norfolk, England. *Proceedings of the Yorkshire Geological Society* **56**: 31–39.
- Peacock JD 1968. *The Geology of the Elgin District*. Geological Survey Scotland, HMSO.
- Peacock JD. 1999. The pre-Windermere Interstadial (Late Devensian) raised marine strata of Eastern Scotland and their macrofauna: a review. *Quaternary Science Reviews* **18**: 1655–1680.
- Peacock JD. 2002. Macrofauna and palaeoenvironment of marine strata of Windermere Interstadial age on the east coast of Scotland. *Scottish Journal of Geology* **38**: 31–40.
- Peacock JD, Browne MAE. 1998. Radiocarbon dates from the Errol Beds (pre-Windermere Interstadial raised marine deposits) in eastern Scotland. *Quaternary Newsletter* **86**: 1–7.
- Peacock JD, Merritt JW. 2000. Glacial deposits at the Boyne Bay Limestone Quarry, Portsoy, and their place in the late Pleistocene history of northeast Scotland. *Journal of Quaternary Science* **15**: 543–555.
- Penny LF, Coope GR, Catt JA. 1969. Age and insect fauna of the Dimlington silts, East Yorkshire. *Nature* **224**: 65–67.
- Phillips ER, Cotterill C, Johnson K *et al.* 2017. Large-scale glacioteconic deformation in response to active ice sheet retreat across Dogger Bank (southern central North Sea) during the Last Glacial Maximum. *Quaternary Science Reviews* **179**: 24–47.
- Plater AJ, Ridgway J, Rayner B *et al.* 2000. Sediment provenance and flux in the Tees Estuary: the record from the Late Devensian to the present. *Geological Society, London, Special Publications* **166**: 171–195.
- Powell RD. 1990. Glacimarine processes at grounding line fans and their growth to ice contact deltas. In *Glacimarine Environments: Processes and Sediments*, Dowdeswell JA, Scourse JD (eds). Geological Society Special Publication: London; 53–73.
- Prescott JR, Hutton JT. 1994. Cosmic ray contributions to dose rates for luminescence and ESR: large depths and long-term time variations. *Radiation Measurements* **23**: 497–500.
- Reimer P, Bard E, Bayliss A, Beck J, Blackwell P, Ramsey C, Van, der Plicht J. 2013. IntCal13 and marine13 radiocarbon age calibration curves 0–50,000 years cal BP. *Radiocarbon* **55**: 1869–1887.
- Roberts DH, Evans DJA, Lodwick J *et al.* 2013. The subglacial and ice-marginal signature of the North Sea lobe of the British Irish Ice Sheet during the last glacial maximum at Uppang, North Yorkshire, UK. *Proceedings of the Geologists' Association* **124**: 503–519.
- Roberts DH, Evans DJA, Callard SL *et al.* 2018. The MIS II limit of the British–Irish Ice Sheet in the Southern North Sea. *Quaternary Science Reviews* **198**: 181–207.
- Roberts DH, Grimoldi E, Callard L *et al.* 2019. The mixed-bed glacial landform imprint of the North Sea Lobe in the western North Sea. *Earth Surface Processes and Landforms* **44**: 1233–1258.
- Rose J. 1985. The Dimlington stadial/Dimlington chronozone: a proposal for naming the main glacial episode of the Late Devensian in Britain. *Boreas* **14**: 225–230.
- Sejrup HP, Hafliðason H, Aarseth I *et al.* 1994. Late Weichselian glaciation history of the northern North Sea. *Boreas* **23**: 1–13.
- Sejrup HP, Larsen E, Landvik J *et al.* 2000. Quaternary glaciations in southern Fennoscandia: evidence from southwestern Norway and the northern North Sea region. *Quaternary Science Reviews* **19**: 667–685.
- Sejrup HP, Nygård A, Hall AM *et al.* 2009. Middle and Late Weichselian (Devensian) glaciation history of south-western Norway, North Sea and eastern UK. *Quaternary Science Reviews* **28**: 370–380.
- Sejrup HP, Hjelstuen BO, Nygård A *et al.* 2015. Late Devensian ice marginal features in the central North Sea—Processes and chronology. *Boreas* **44**: 1–13.
- Sejrup HP, Clark CD, Hjelstuen BO. 2016. Rapid ice sheet retreat triggered by ice stream debudding: Evidence from the North Sea. *Geology* **44**: 355–358.
- Shennan I, Bradley S, Milne G *et al.* 2006. Relative sea-level changes, glacial isostatic modelling and ice-sheet reconstructions from the British Isles since the Last Glacial Maximum. *Journal of Quaternary Science* **21**: 585–599.
- Shennan I, Bradley SL, Edwards R. 2018. Relative sea-level changes and crustal movements in Britain and Ireland since the Last Glacial Maximum. *Quaternary Science Reviews* **188**: 143–159.
- Sissons JB. 1963. The Perth readvance in central Scotland. Part I. *Scottish Geographical Magazine* **79**: 151–163.
- Sissons JB. 1971. The geomorphology of central Edinburgh. *Scottish Geographical Magazine* **87**: 185–196.
- Smith DB. 1981. The Quaternary Geology of the Sunderland District, north-east England. In *The Quaternary in Britain*, Neale J, Flenley J (eds). Pergamon: Oxford; 146–167.
- Staines KEH 2009. The glacial geomorphology of the Tweed valley and surrounding area, eastern British Isles. Unpublished MSc thesis, Durham University.
- Stoker MS, Long D, Fyfe JA 1985. *A revised Quaternary stratigraphy for the central North Sea*. British Geological Survey.
- Straw A. 1957. Some glacial features of East Lincolnshire. *East Midlands Geographer* **1**: 41–48.
- Straw A. 1958. The glacial sequence in Lincolnshire. *East Midlands Geographer* **2**: 29–40.
- Straw A. 1960. The limit of the blastQ glaciation in North Norfolk. *Proceedings of the Geologists' Association* **71**: 379–390.

- Straw A. 1961. Drifts, meltwater channels and ice margins in the Lincolnshire Wolds. *Transactions of the Institute of British Geographers* **29**: 115–128.
- Straw A. 1979. The Devensian glaciation. In *The Geomorphology of the British Isles: Eastern and Central England*, Straw A, Clayton KM (eds). Methuen: London; 21–45.
- Suggate RP, West RG 1959. On the extent of the last glaciation in eastern England. *Proceedings of the Royal Society B* **150**: 263–283.
- Sutherland DG. 1984. The Quaternary deposits and landforms of Scotland and the neighbouring shelves—a review. *Quaternary Science Reviews* **3**: 157–254.
- Synge FM. 1956. The glaciation of north-east Scotland. *Scottish Geographical Magazine* **72**: 129–143.
- Synge FM 1963. The Quaternary succession around Aberdeen, north-east Scotland. Report of the VI INQUA Congress, Warsaw, vol. 3, pp. 353–360.
- Teasdale D. 2013. Evidence for the western limits of the North Sea Lobe of the BIIS in North East England. In *The Quaternary of Northumberland, Durham and Yorkshire Field Guide*, Davies BJ, Yorke L, Bridgland DR et al. (eds). Quaternary Research Association: London; 106–121.
- Thomas GSP 1999. Northern England. In *A revised correlation of Quaternary deposits in the British Isles*, Bowen DQ (ed). Geological Society Special Report 23: 91–98.
- Thomsen KJ, Murray AS, Bøtter-Jensen L et al. 2007. Determination of burial dose in incompletely bleached fluvial samples using single grains of quartz. *Radiation Measurements* **42**: 370–379.
- Thomson ME, Eden RA 1977. Quaternary deposits of the central North Sea: 3. The Quaternary sequence in the west central North Sea. Institute of Geological Sciences.
- Waelbroeck C, Labeyrie L, Michela E et al. 2002. Sea-level and deep water temperature changes derived from benthic foraminifera isotopic records. *Quaternary Science Reviews* **21**: 295–305.
- Yorke L, Rumsby BT, Chiverrell RC. 2012. Depositional history of the Tyne valley associated with retreat and stagnation of Late Devensian Ice Streams. *Proceedings of the Geologists' Association* **123**: 608–625.